

SAR Interferometry: Theory

Tim J Wright

COMET, School of Earth and Environment,
University of Leeds, UK

1–5 July 2013 | Harokopio University | Athens, Greece

Outline

PART 1: InSAR – the basics

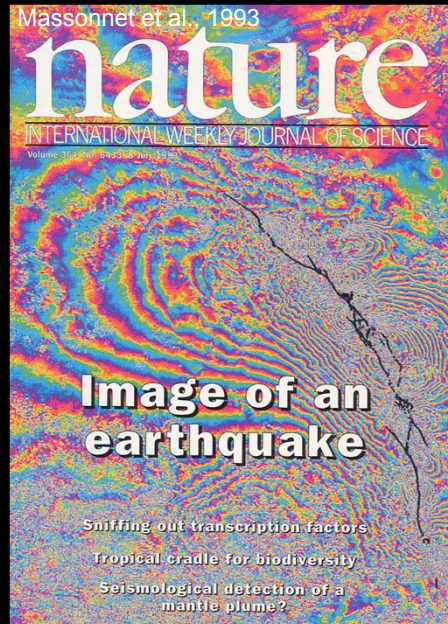
- Components of interferometric phase
- Error Budget for single Interferogram

PART 2: InSAR – “advanced” methods

- Time Series Methods
- Determining 3D displacements
- Correcting Atmospheric Noise

InSAR – how it works

- Actively illuminate ground with radar waves.
- Operates day and night, can see through clouds
- ERS, Envisat (1991): very stable orbits and pointing
⇒ InSAR
- Followed by ERS-2 (1995) and Envisat (2003) for ~ 20 year time series

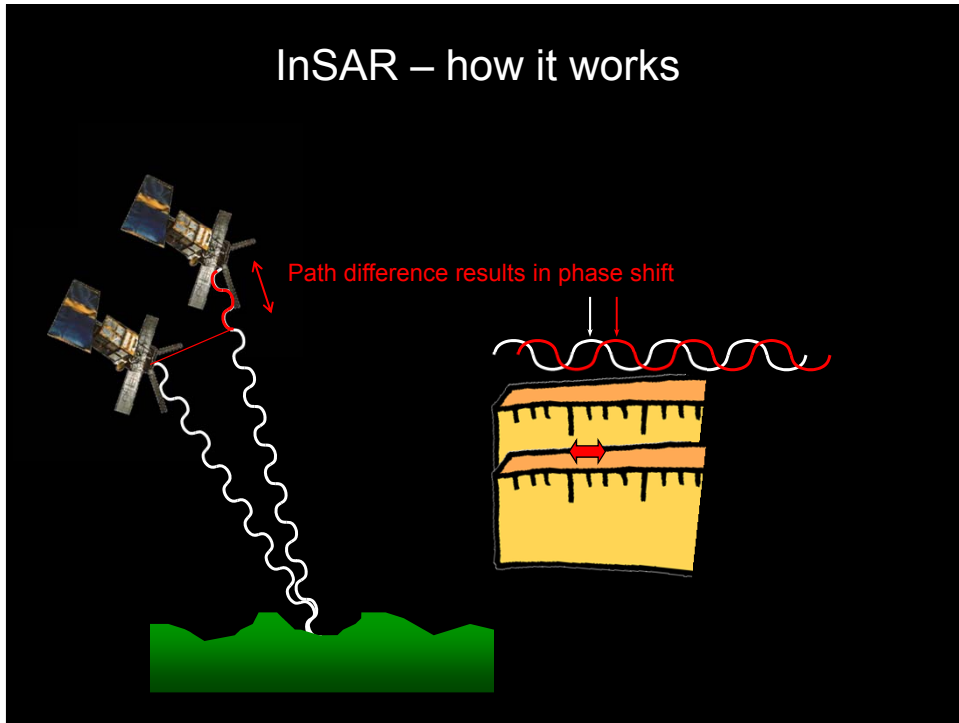


InSAR – how it works

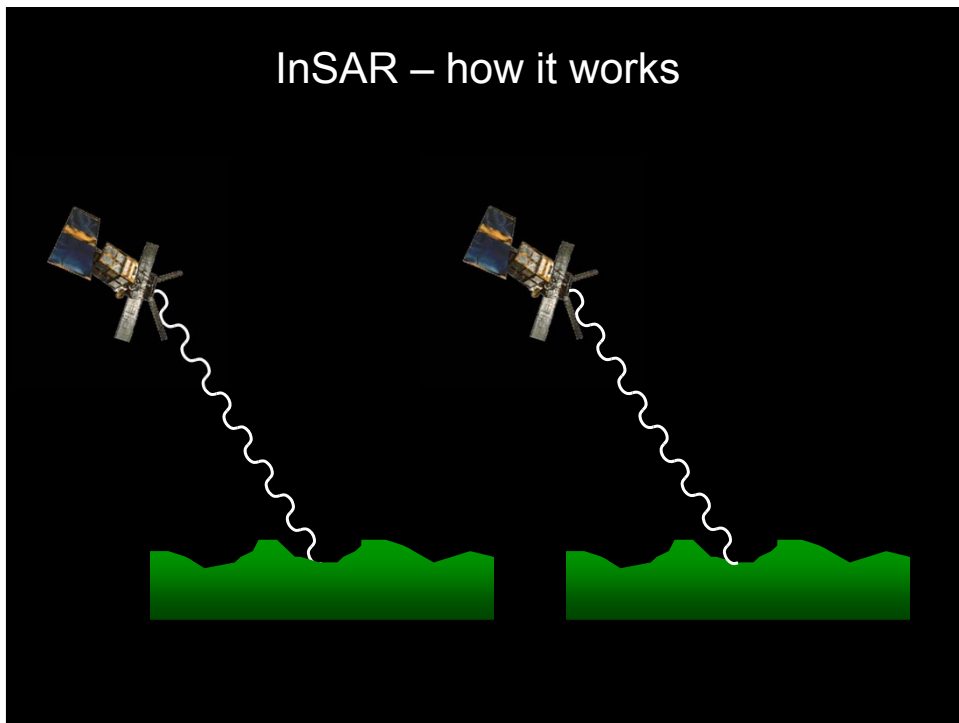
Round trip ~ 30 million wavelengths
BUT we don't know the exact number



InSAR – how it works



InSAR – how it works



InSAR – how it works

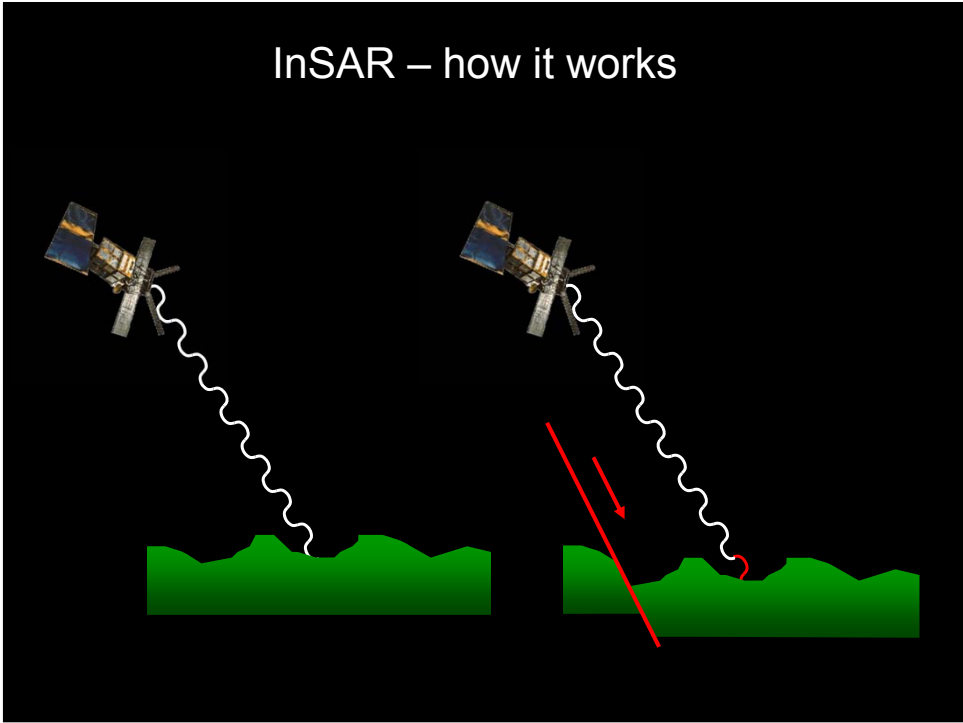
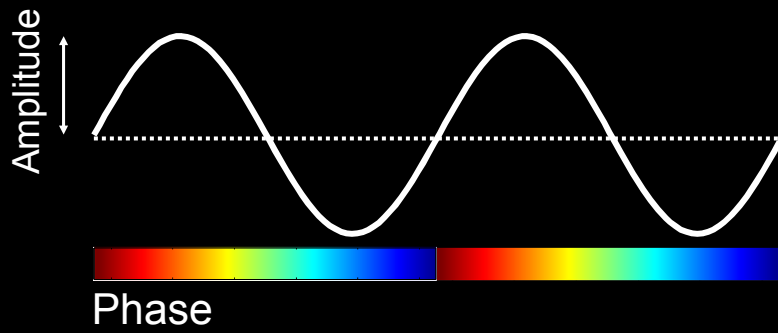
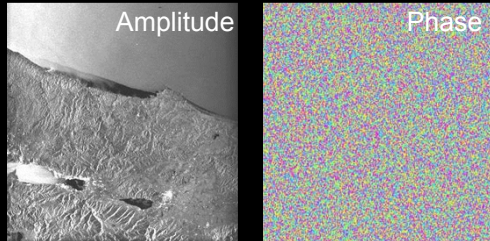
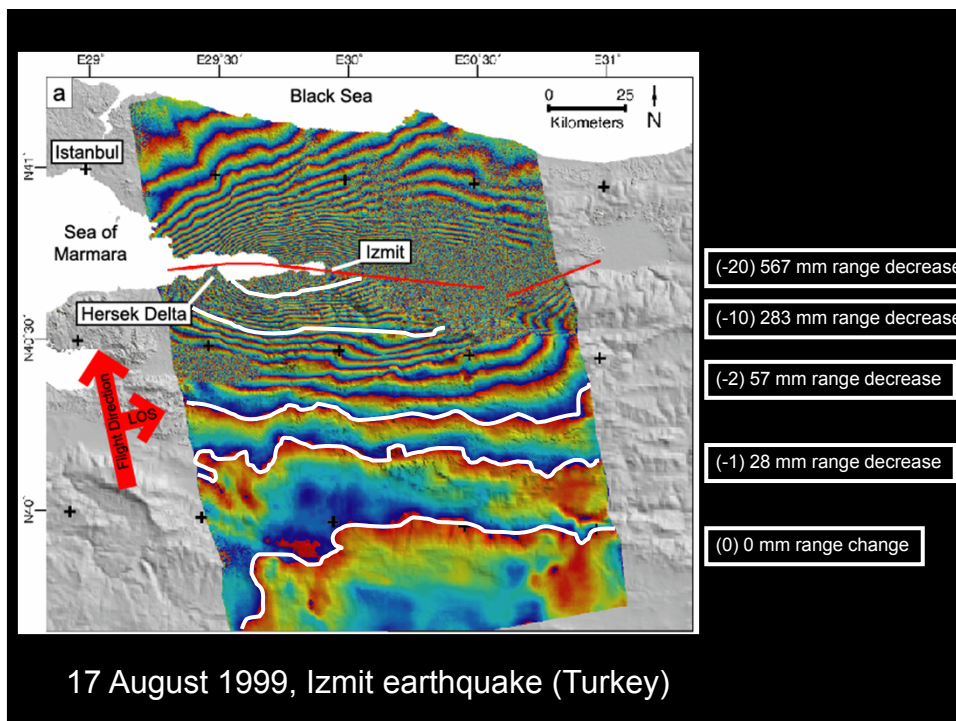
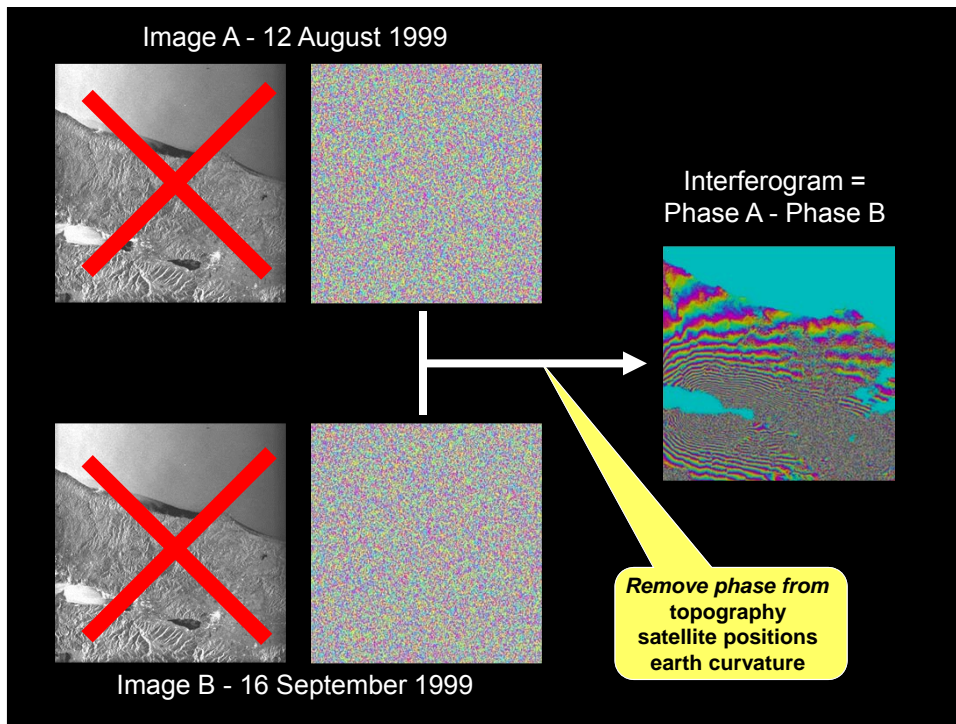
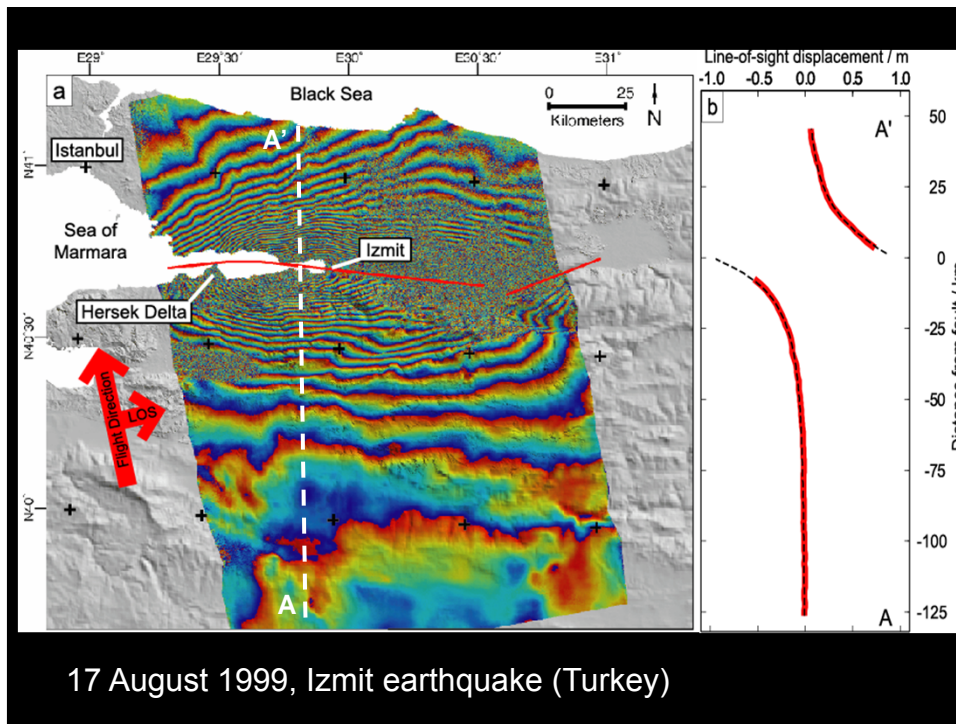


Image A - 12 August 1999





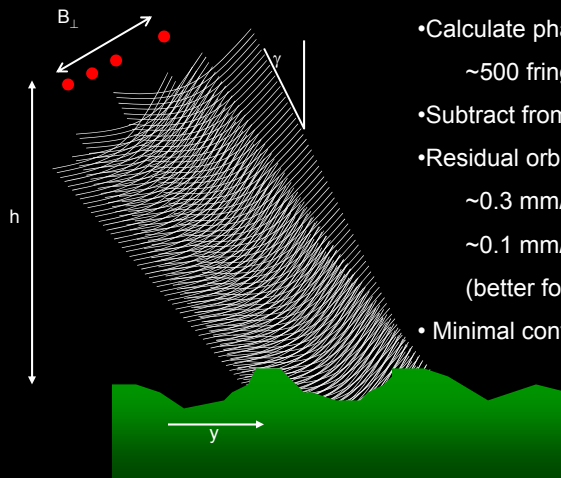


Components of interferometric phase

$$\Delta\phi_{\text{int}} = \cancel{\Delta\phi_{\text{geom}}} + \cancel{\Delta\phi_{\text{topo}}} + \cancel{\Delta\phi_{\text{atm}}} + \cancel{\Delta\phi_{\text{noise}}} + \Delta\phi_{\text{def}}$$

Components of interferometric phase

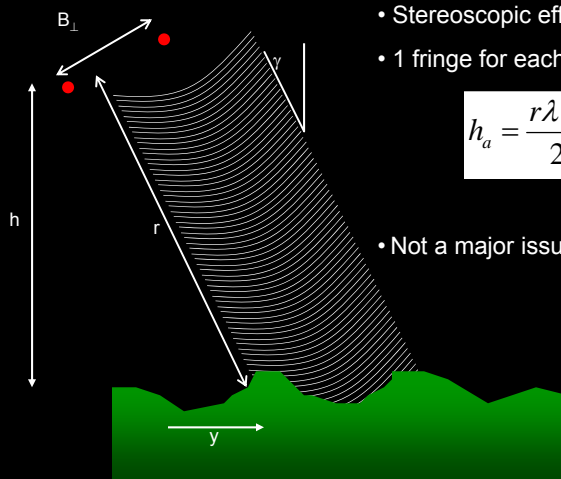
$$\Delta\phi_{\text{int}} = \Delta\phi_{\text{geom}} + \Delta\phi_{\text{topo}} + \Delta\phi_{\text{atm}} + \Delta\phi_{\text{noise}} + \Delta\phi_{\text{def}}$$



- Calculate phase ramp from satellite orbits
~500 fringes across typical frame
- Subtract from interferogram
- Residual orbital errors:
~0.3 mm/km (north, ERS)
~0.1 mm/km (east, ERS)
(better for Envisat)
- Minimal control on v. long wavelength

Components of interferometric phase

$$\Delta\phi_{\text{int}} = \Delta\phi_{\text{geom}} + \Delta\phi_{\text{topo}} + \Delta\phi_{\text{atm}} + \Delta\phi_{\text{noise}} + \Delta\phi_{\text{def}}$$



- Stereoscopic effect \Rightarrow topographic fringes
- 1 fringe for each change in elevation h_a

$$h_a = \frac{r\lambda \sin \gamma}{2B_{\perp}} \approx \frac{10,000}{B_{\perp}}$$

- Not a major issue since SRTM

Components of interferometric phase

$$\Delta\phi_{\text{int}} = \Delta\phi_{\text{geom}} + \Delta\phi_{\text{topo}} + \Delta\phi_{\text{atm}} + \Delta\phi_{\text{noise}} + \Delta\phi_{\text{def}}$$

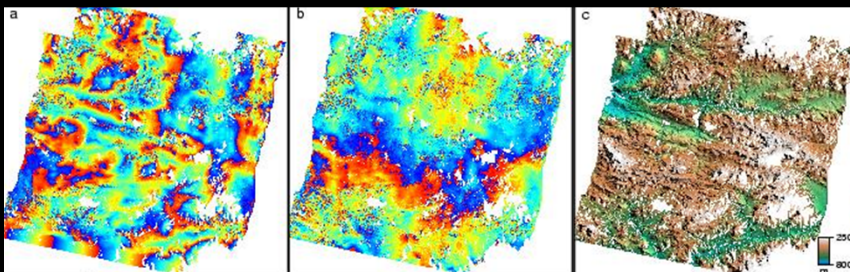


A foggy morning,
near ancient Mycenae,
Greece

Components of interferometric phase

$$\Delta\phi_{\text{int}} = \Delta\phi_{\text{geom}} + \Delta\phi_{\text{topo}} + \Delta\phi_{\text{atm}} + \Delta\phi_{\text{noise}} + \Delta\phi_{\text{def}}$$

Layered atmosphere



29/8/1995 to 29/7/1997

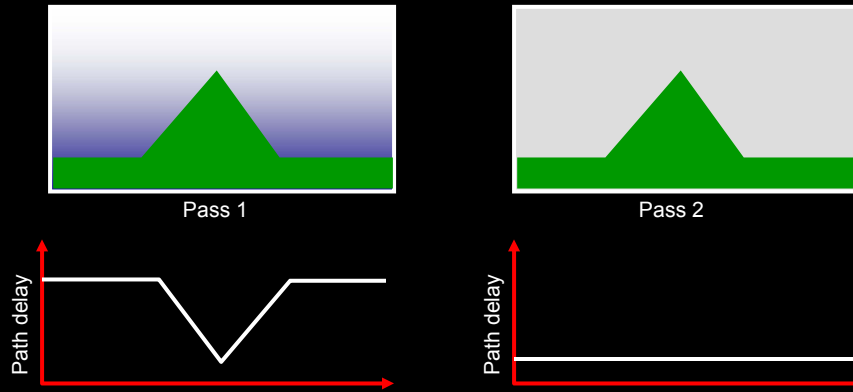
30/8/1995 to 29/7/1997

Topography

Components of interferometric phase

$$\Delta\phi_{\text{int}} = \Delta\phi_{\text{geom}} + \Delta\phi_{\text{topo}} + \Delta\phi_{\text{atm}} + \Delta\phi_{\text{noise}} + \Delta\phi_{\text{def}}$$

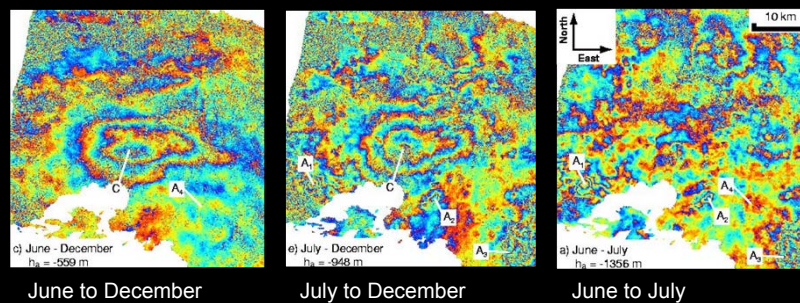
Layered atmosphere



Components of interferometric phase

$$\Delta\phi_{\text{int}} = \Delta\phi_{\text{geom}} + \Delta\phi_{\text{topo}} + \Delta\phi_{\text{atm}} + \Delta\phi_{\text{noise}} + \Delta\phi_{\text{def}}$$

Turbulent atmosphere



Athens Earthquake – September 1999

Components of interferometric phase

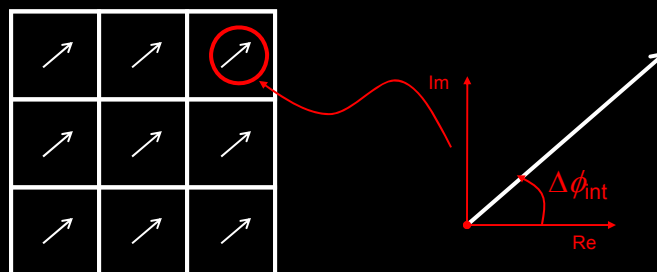
$$\Delta\phi_{\text{int}} = \Delta\phi_{\text{geom}} + \Delta\phi_{\text{topo}} + \Delta\phi_{\text{atm}} + \Delta\phi_{\text{noise}} + \Delta\phi_{\text{def}}$$

- Size of $\Delta\phi_{\text{atm}}$ (at sea level) scales with distance, but can be +/- 10 cm or more.
- Methods for dealing with $\Delta\phi_{\text{atm}}$
 - Ignore (most common)
 - Quantify
 - Model based on other observations (e.g. GPS, meteorology...)
 - Increase SNR by stacking or time series analysis

Components of interferometric phase

$$\Delta\phi_{\text{int}} = \Delta\phi_{\text{geom}} + \Delta\phi_{\text{topo}} + \Delta\phi_{\text{atm}} + \Delta\phi_{\text{noise}} + \Delta\phi_{\text{def}}$$

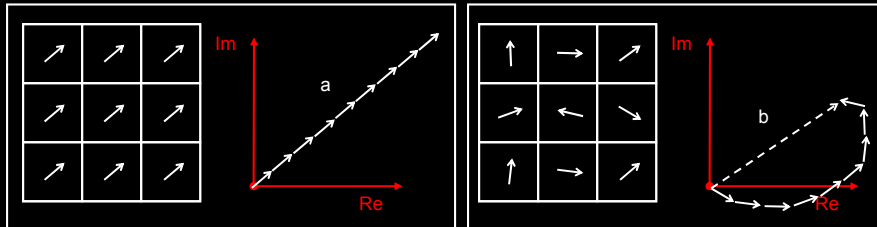
- Biggest source of noise is due to changing ground surface
- *Coherence* is convenient measure



Components of interferometric phase

$$\Delta\phi_{\text{int}} = \Delta\phi_{\text{geom}} + \Delta\phi_{\text{topo}} + \Delta\phi_{\text{atm}} + \Delta\phi_{\text{noise}} + \Delta\phi_{\text{def}}$$

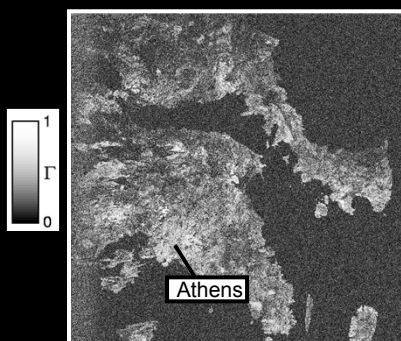
- Biggest source of noise is due to changing ground surface
- *Coherence* is convenient measure



$$\text{Coherence} = b / a$$

Components of interferometric phase

$$\Delta\phi_{\text{int}} = \Delta\phi_{\text{geom}} + \Delta\phi_{\text{topo}} + \Delta\phi_{\text{atm}} + \Delta\phi_{\text{noise}} + \Delta\phi_{\text{def}}$$



Coherent surface types

- Bare Rock
- Buildings esp. towns/cities

- Grassland
- Agricultural fields
- Ice

Incoherent surface types

- Leafy Trees
- Water

Components of interferometric phase

$$\Delta\phi_{\text{int}} = \Delta\phi_{\text{geom}} + \Delta\phi_{\text{topo}} + \Delta\phi_{\text{atm}} + \Delta\phi_{\text{noise}} + \Delta\phi_{\text{def}}$$

1. incoherence

- Changes in the ground cover cause a random phase shift for each pixel
- Large baselines

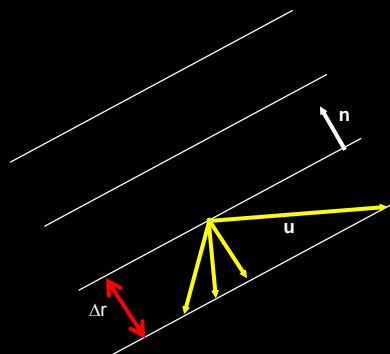
2. Unwrapping errors

- Phase in interferograms is wrapped (each fringe is 2π radians).
- Discontinuities or data gaps can cause phase unwrapping errors

Components of interferometric phase

$$\Delta\phi_{\text{int}} = \Delta\phi_{\text{geom}} + \Delta\phi_{\text{topo}} + \Delta\phi_{\text{atm}} + \Delta\phi_{\text{noise}} + \Delta\phi_{\text{def}}$$

InSAR ONLY MEASURES THE COMPONENT OF SURFACE DEFORMATION IN THE SATELLITE'S LINE OF SIGHT



$$\Delta r = -n \cdot u$$

where n is a unit vector pointing from the ground to the satellite

$$\Delta\phi_{\text{def}} = (4\pi / \lambda) \Delta r$$

i.e. 1 fringe = 28.3 mm l.o.s. deformation for ERS

Error Budget (1)

Single interferogram

$$\sigma_{def}^2 = \sigma_{gm}^2 + \sigma_{topo}^2 + \sigma_{atm}^2 + \sigma_{coh}^2 + \sigma_{sys}^2 + \sigma_{unw}^2$$

- Orbital errors \Rightarrow long-wavelength ramps.
- Envisat: ~ 0.3 mm/km (across-track) and 0.1 mm/km (along-track) [Wang, Wright and Biggs, GRL 2009].
- Can correct by processing long strips and tying to GPS (see. Fringe presentations by Wang, Pagli and Hamlyn)
- Should be negligible for future missions with onboard GPS receivers.

Error Budget (1)

Single interferogram

$$\sigma_{def}^2 = \sigma_{gm}^2 + \sigma_{topo}^2 + \sigma_{atm}^2 + \sigma_{coh}^2 + \sigma_{sys}^2 + \sigma_{unw}^2$$

$$\sigma_{topo} = \frac{\bar{r}_{slant} B_{\perp}}{\sin \theta_{inc}} \sigma_{DEM}$$

- SRTM error ~ 4 m absolute, of which 2.5 m is not spatially correlated [Rodriguez et al., PERS 2006]

B_{perp}	σ_{topo} (40° incidence)
150 m	1.1 mm
300 m	2.3 mm
1000 m	7.8 mm

Error Budget (1) Single interferogram

$$\sigma_{def}^2 = \sigma_{gm}^2 + \sigma_{topo}^2 + \sigma_{atm}^2 + \sigma_{coh}^2 + \sigma_{sys}^2 + \sigma_{unw}^2$$

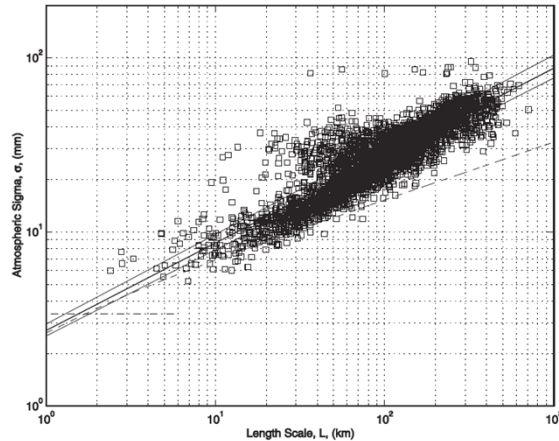
- Troposphere

Emardson et al., 2003:

$$\sigma = cL^\alpha \quad [c \sim 2.5, \alpha \sim 0.5]$$

$$\sigma = 25 \text{ mm at } 100 \text{ km}$$

(assume no corrections)



Error Budget (1) Single interferogram

$$\sigma_{def}^2 = \sigma_{gm}^2 + \sigma_{topo}^2 + \sigma_{atm}^2 + \sigma_{coh}^2 + \sigma_{sys}^2 + \sigma_{unw}^2$$

- Ionosphere ($1/f^2$ dependence). Important at L-band, but not at C-band.
- Can correct with split band processing (e.g. 1200 and 1260 MHz) in future missions
- Ionospheric error on 100 km wavelength \sim 1mm after spatial averaging

Error Budget (1)

Single interferogram

$$\sigma_{def}^2 = \sigma_{gm}^2 + \sigma_{topo}^2 + \sigma_{atm}^2 + \sigma_{coh}^2 + \sigma_{sys}^2 + \sigma_{unw}^2$$

- Coherence, γ
 - important at short wavelengths, but can be averaged through multilooking to < 1 mm for most ground cover types

Error Budget (1)

Single interferogram

$$\sigma_{def}^2 = \sigma_{gm}^2 + \sigma_{topo}^2 + \sigma_{atm}^2 + \sigma_{coh}^2 + \sigma_{sys}^2 + \sigma_{unw}^2$$

- Coherence, γ
 - important at short wavelengths, but can be averaged through multilooking to < 1 mm for most ground cover types
- System (thermal) - modifies coherence
 - reduces effective coherence, but still insignificant after spatial averaging.

$$\sigma_{coh} = \left(\frac{\lambda}{4\pi} \right) \frac{1}{\sqrt{N_L}} \frac{\sqrt{1-\gamma^2}}{\gamma}$$

$$\gamma_c = \frac{\gamma}{1 + SNR^{-1}}$$

Error Budget (1)

Single interferogram

$$\sigma_{def}^2 = \sigma_{gm}^2 + \sigma_{topo}^2 + \sigma_{atm}^2 + \sigma_{coh}^2 + \sigma_{sys}^2 + \sigma_{unw}^2$$

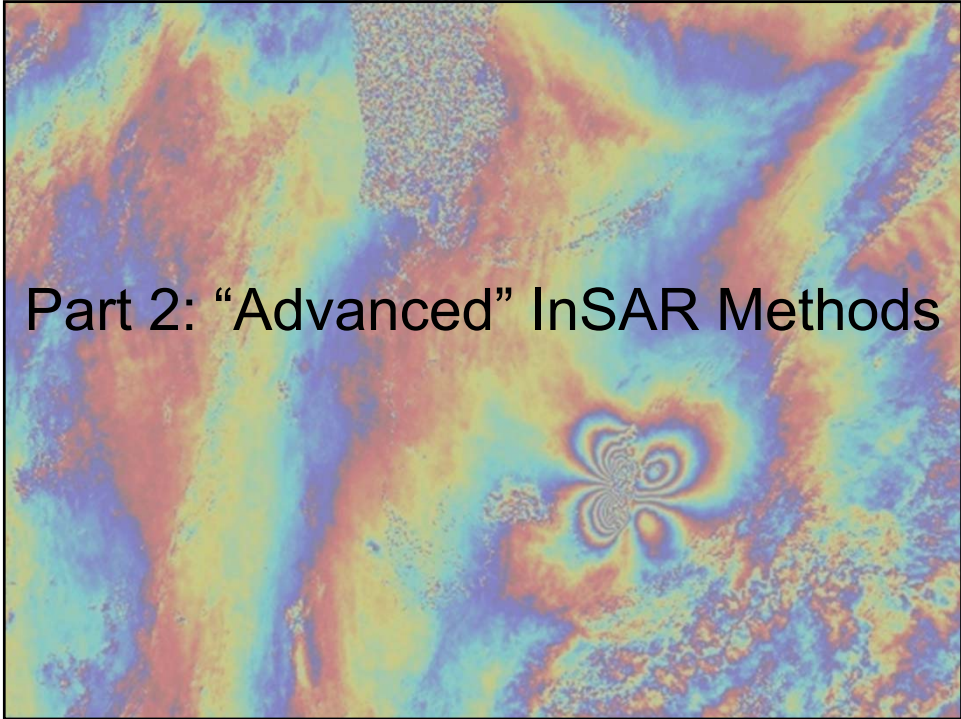
- Unwrapping errors difficult to quantify.
- Assume = 0 in this analysis (probably OK for L-band missions or missions with short revisits).

Error Budget (1)

Single interferogram

$$\sigma_{def}^2 = \sigma_{gm}^2 + \sigma_{topo}^2 + \sigma_{atm}^2 + \sigma_{coh}^2 + \sigma_{sys}^2 + \sigma_{unw}^2$$

Atmospheric (tropospheric) error dominates at 100 km length scales, at which single interferograms have error of ~25 mm.

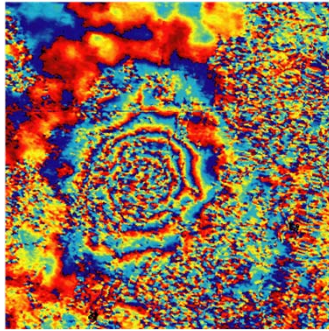


Part 2: “Advanced” InSAR Methods

Outline for Advanced Methods

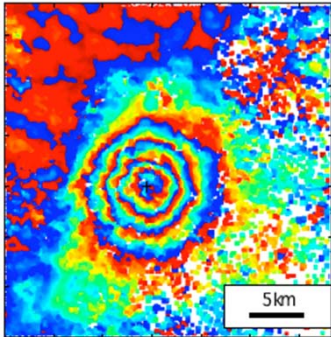
1. Combining interferograms
 - Stacking
 - Time series
 - SBAS/Permanent Scatterers
 - Error budget for Time Series Methods
2. Determining 3D displacements/velocities
 - Direct inversion
 - Combination with GPS
3. Atmospheric Corrections
 - Linear/Smooth Velocity Assumption
 - MERIS/MODIS
 - GPS
 - Weather Models

Stacking



Individual Interferogram

Typical atmospheric noise for individual interferogram ~ 1 cm



Stack of 5 images

Stack: Add together 5 interferograms

Signal increases by a factor of 5

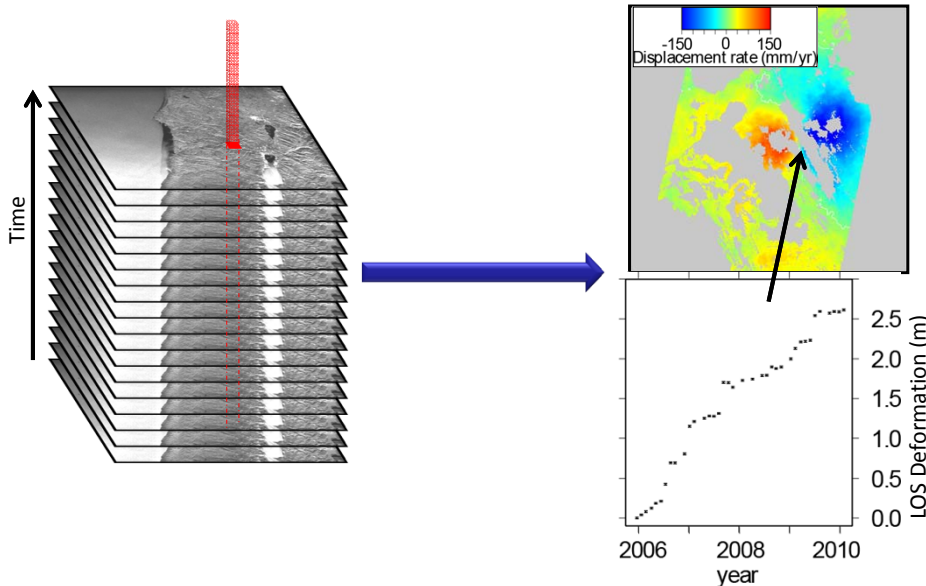
Noise increases by a factor of $\sqrt{5}$

Signal:Noise ratio increases by $5/\sqrt{5} = \sqrt{5} \sim 2.23$

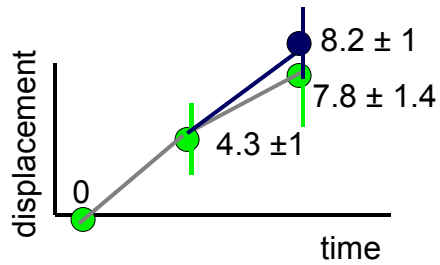
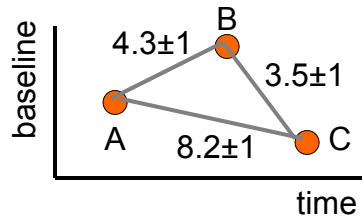
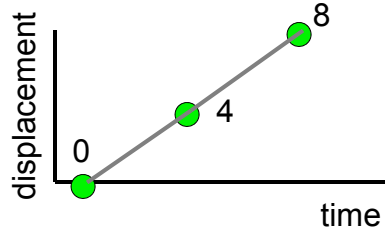
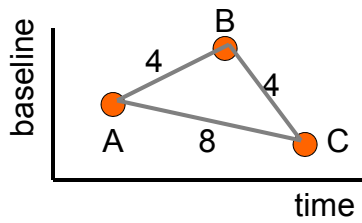
For continuous phenomena (e.g. interseismic strain) or discrete events (e.g. earthquakes)

Biggs et al, 2009 (Geology)

All time series methods are essentially the same – rely on large stacks of imagery to separate signal from noise



Time Series Example



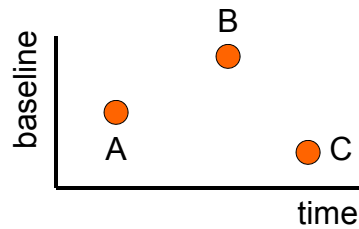
Time Series Inversion

Acquisitions A,B,C

$$i_{AB} = d_B - d_A = v_{AB} t_{AB}$$

$$i_{BC} = d_C - d_B = v_{BC} t_{BC}$$

$$i_{AC} = d_C - d_A = (d_C - d_B) + (d_B - d_A) = v_{AB} t_{AB} + v_{BC} t_{BC}$$



$$\begin{bmatrix} t_{AB} & 0 \\ 0 & t_{BC} \\ t_{AB} & t_{BC} \end{bmatrix} \begin{bmatrix} v_{AB} \\ v_{BC} \end{bmatrix} = \begin{bmatrix} i_{AB} \\ i_{BC} \\ i_{AC} \end{bmatrix}$$

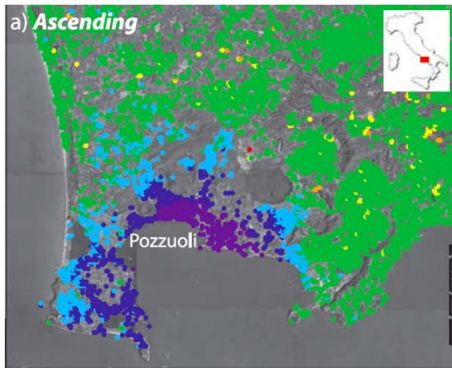
$$\boxed{G_{INS} m = d_{INS}}$$

To get correct answer with this method, weighting with covariances is essential

$$\boxed{\Sigma^{-1} G_{INS} m = \Sigma^{-1} d_{INS}}$$

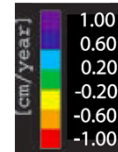
SBAS: Short BAseline Subset

Example: Campi Flegrei caldera (Italy).



30 ascending images
=> 180 interferograms

Max uplift of 2 cm/yr in
Pozzuoli Harbour

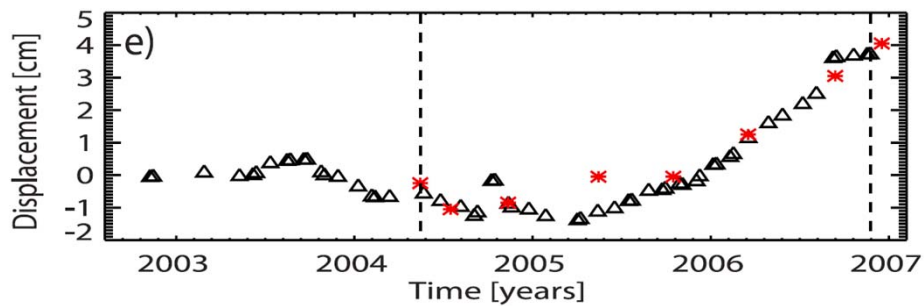


Modelled by an inflation rate of
a magma chamber at a depth
of 3.2 km with a volume change
of $1.1 \times 10^6 \text{ m}^3/\text{yr}$

(Trasatti et al, 2008; Casu et al, 2006)

SBAS

Pozzuoli Harbour time series:

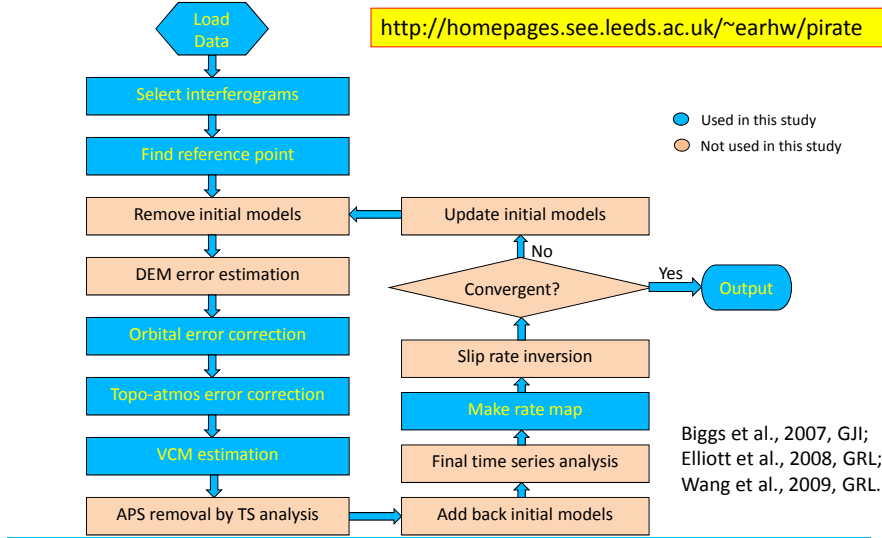


Stated accuracy: 1 mm/yr in rate. 5 mm in displacement.

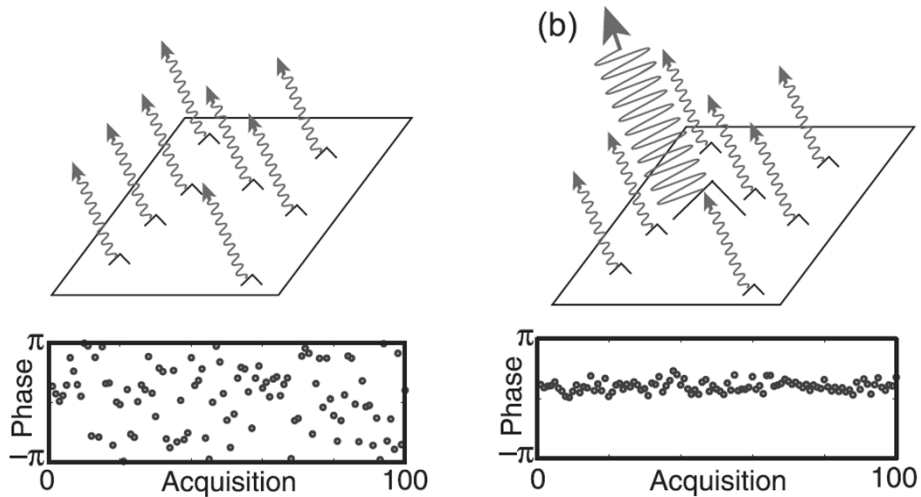
Good match with levelling data (red).

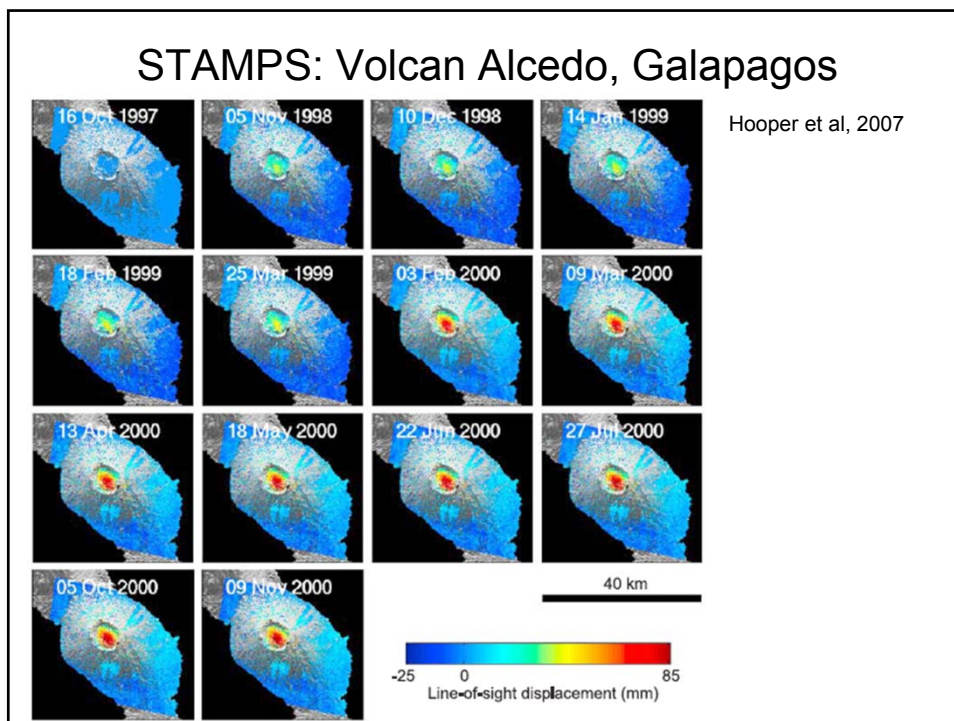
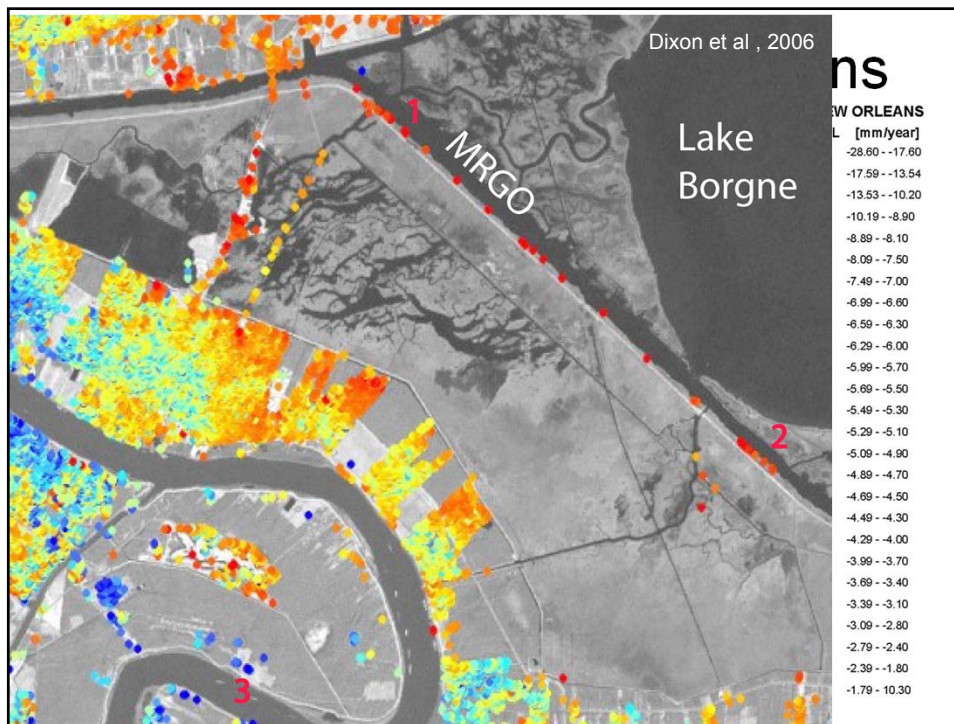
PI-RATE: Poly-Interferogram Rate And Time-series Estimator

<http://homepages.see.leeds.ac.uk/~earhw/irate>



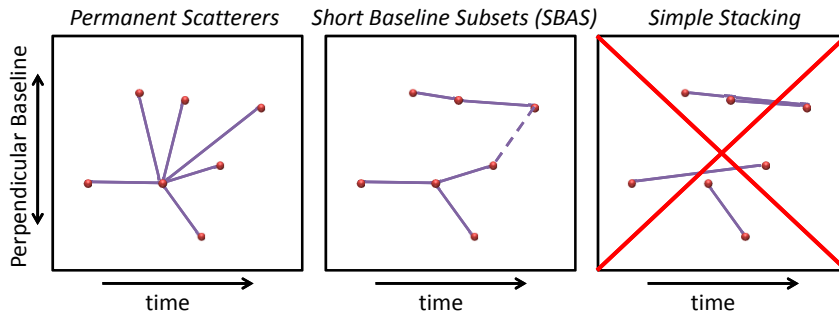
PS InSAR:





Error Budget (2)

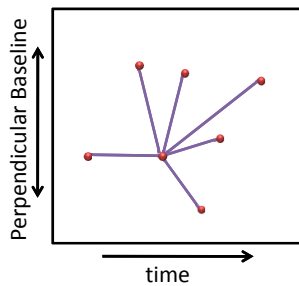
Optimum determination of Linear Deformation Rates



For the determination of linear deformation rates, optimum errors are determined through a connected network, since noise terms are associated with individual acquisitions not interferograms.

Error Budget (2)

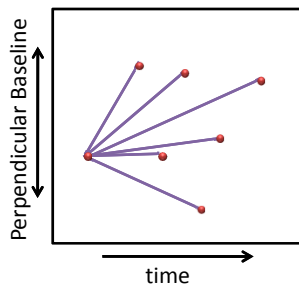
Optimum determination of Linear Deformation Rates



- Error on linear rate is independent of how network is connected (but of course short-baseline, short-time interferograms are best).

Error Budget (2)

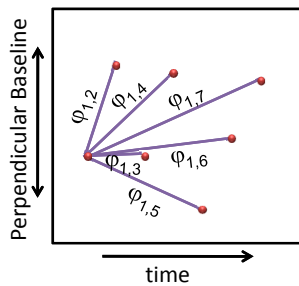
Optimum determination of Linear Deformation Rates



- Error on linear rate is independent of how network is connected (but of course short-baseline, short-time interferograms are best).
- To simplify mathematics, assume all connections to date d_1 ...

Error Budget (2)

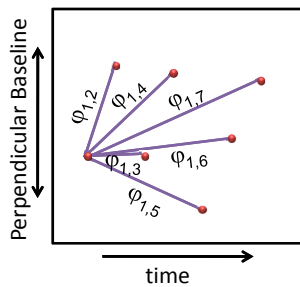
Optimum determination of Linear Deformation Rates



- Error on linear rate is independent of how network is connected (but of course short-baseline, short-time interferograms are best).
- To simplify mathematics, assume all connections to date d_1 ...
...and regular acquisition spacing, t_m

Error Budget (2)

Optimum determination of Linear Deformation Rates



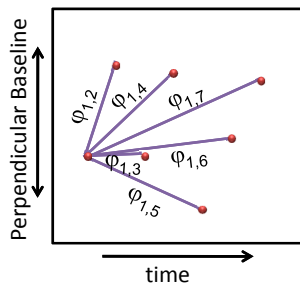
- Error on linear rate is independent of how network is connected (but of course short-baseline, short-time interferograms are best).
- To simplify mathematics, assume all connections to date d1...
...and regular acquisition spacing, t_r
- We can determine the best-fit linear rate of phase change due to deformation, $\frac{d\phi}{dt}$, using weighted least squares:

$$\Sigma_p^{-1} \mathbf{T} \frac{d\phi}{dt} = \Sigma_p^{-1} \mathbf{P}$$

where $\mathbf{T} = [t_r, 2t_r, \dots, Nt_r]^T$, $\mathbf{P} = [\phi_{1,2}, \phi_{1,3}, \dots, \phi_{1,N}]^T$, and Σ_p^{-1} is the inverse of the variance-covariance matrix for the range change observations, \mathbf{P} .

Error Budget (2)

Optimum determination of Linear Deformation Rates



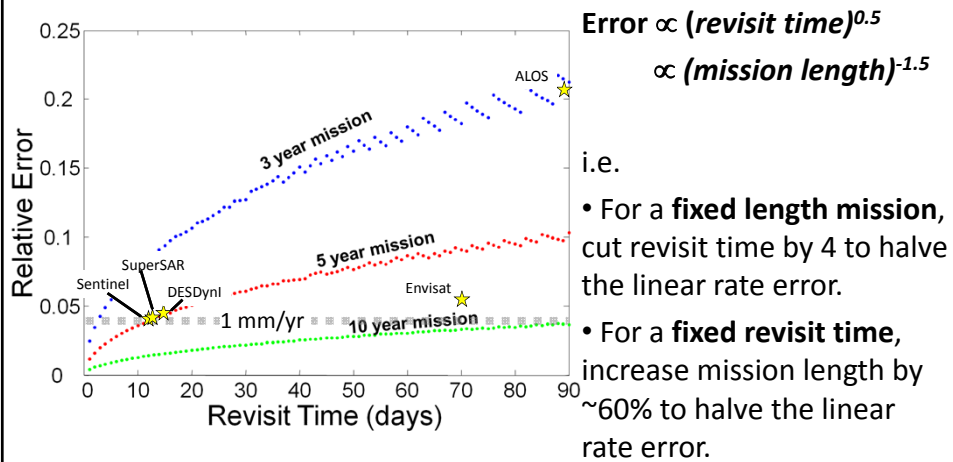
- Using the correct VCM, Σ_p , is essential.
- In this particular network, all interferograms share a common acquisition (epoch 1).

$$\Rightarrow \text{Cov}(\phi_{1,i}, \phi_{1,j}) = \sigma_1^2 \quad (\text{the variance on epoch 1})$$

$$\text{and } \text{Var}(\phi_{1,i}) = \sigma_1^2 + \sigma_i^2 = 2\sigma^2 \quad (\text{assuming noise is identical on all epochs})$$

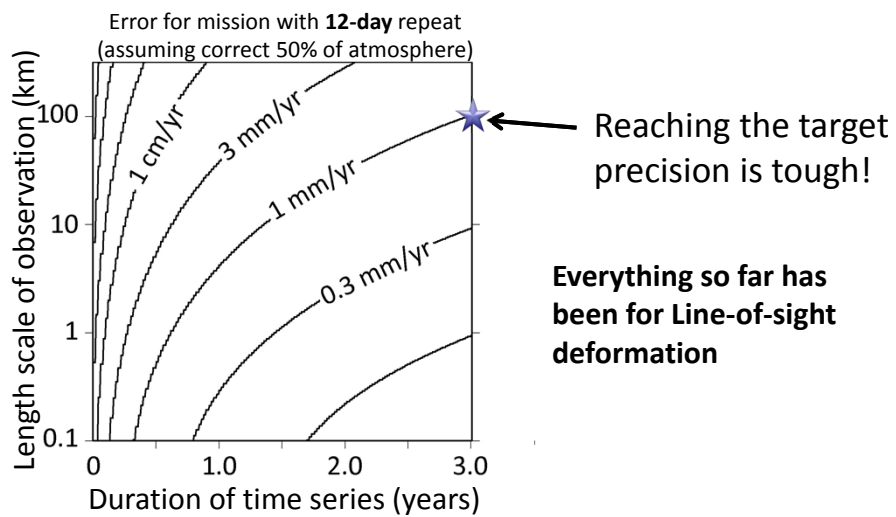
Error Budget (2)

Optimum determination of Linear Deformation Rates

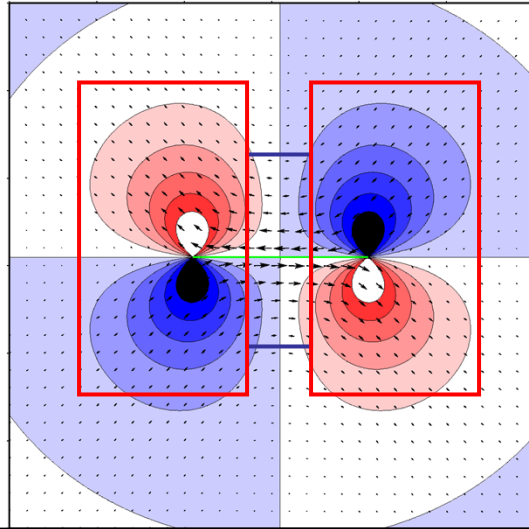


Error Budget (2)

Optimum determination of Linear Deformation Rates



Combining Viewing Geometries

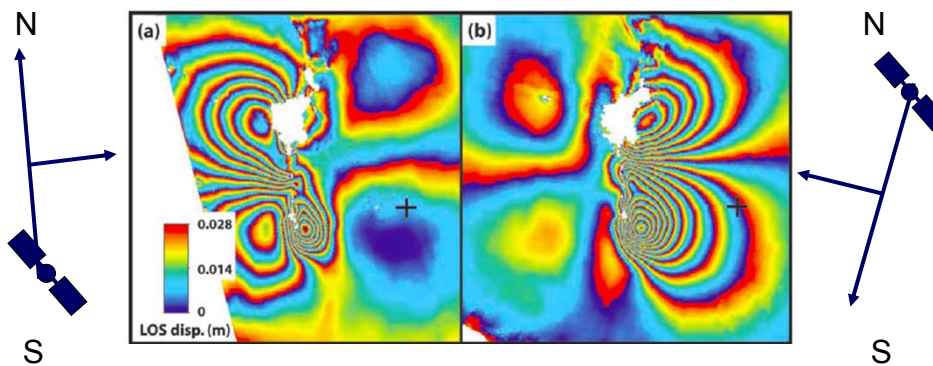


Surface
Displacements
of Strike Slip
Faults

Combining Viewing Geometries

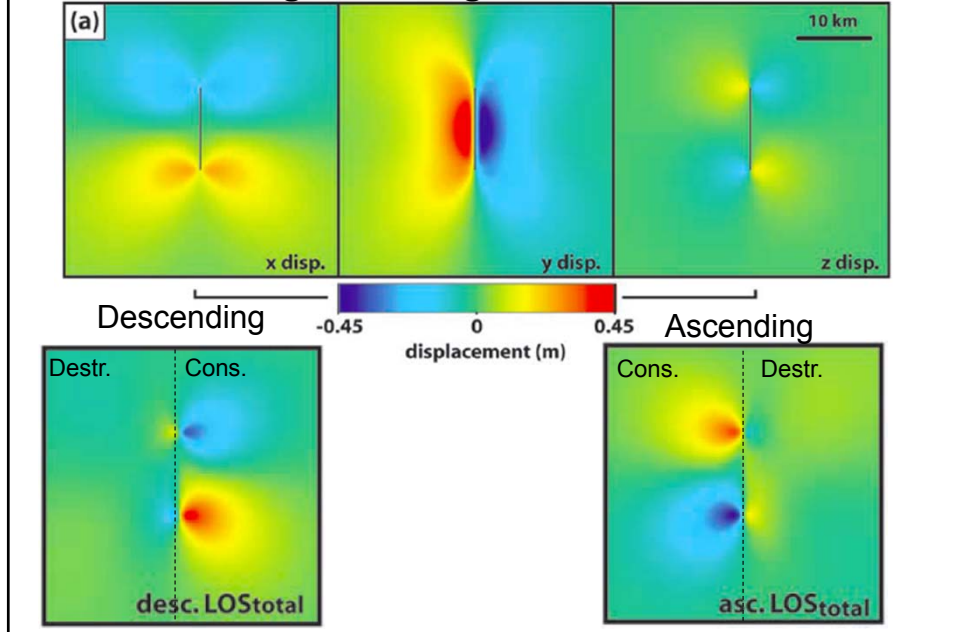
Ascending

Descending

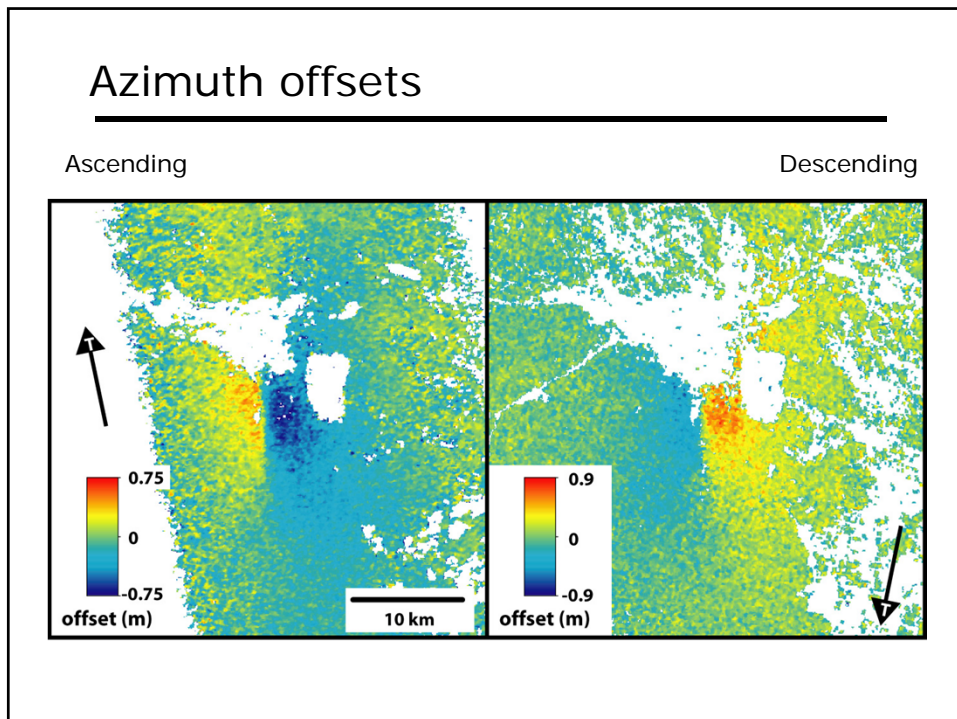


Bam, Earthquake, Iran, 2003. (Funning et al, 2006)

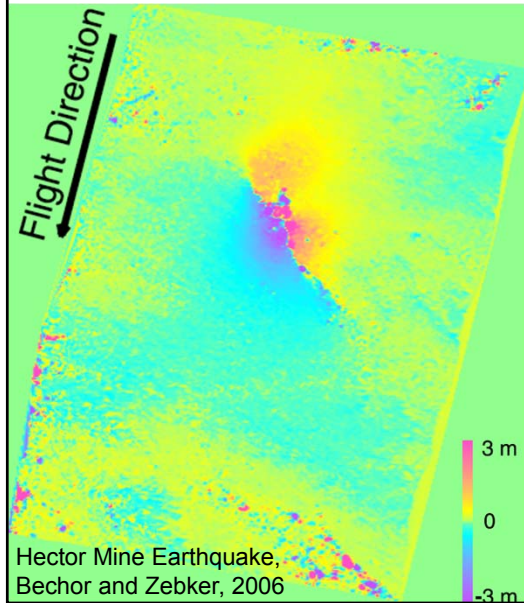
Combining Viewing Geometries



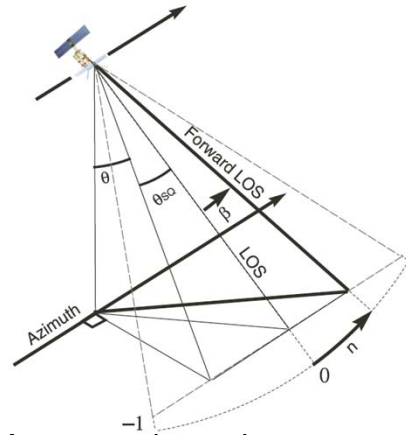
Azimuth offsets



MAI: Split Beam Processing



Split beam into forward- and backward- looking sections to measure displacement in flight direction.



Accuracy depends on coherence and SNR. Up to 3 cm.

Determining 3D displacements

If the 3D displacement at a pixel is given by

$\mathbf{u} = [u_x, u_y, u_z]$, then...

Ascending interferogram, $d_1 = \mathbf{los}_A \cdot \mathbf{u}$

Descending interferogram, $d_2 = \mathbf{los}_D \cdot \mathbf{u}$

Ascending az. offsets, $d_3 = \mathbf{los}_{AO} \cdot \mathbf{u}$

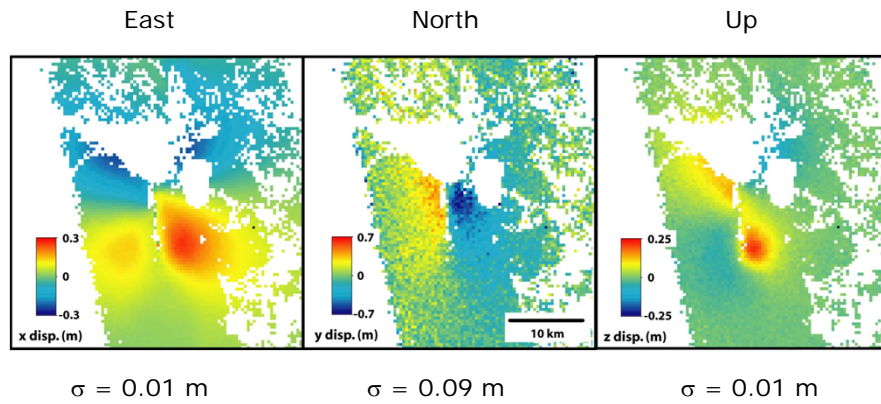
Descending az. offsets, $d_4 = \mathbf{los}_{DO} \cdot \mathbf{u}$

Which can be rewritten as a matrix equation,

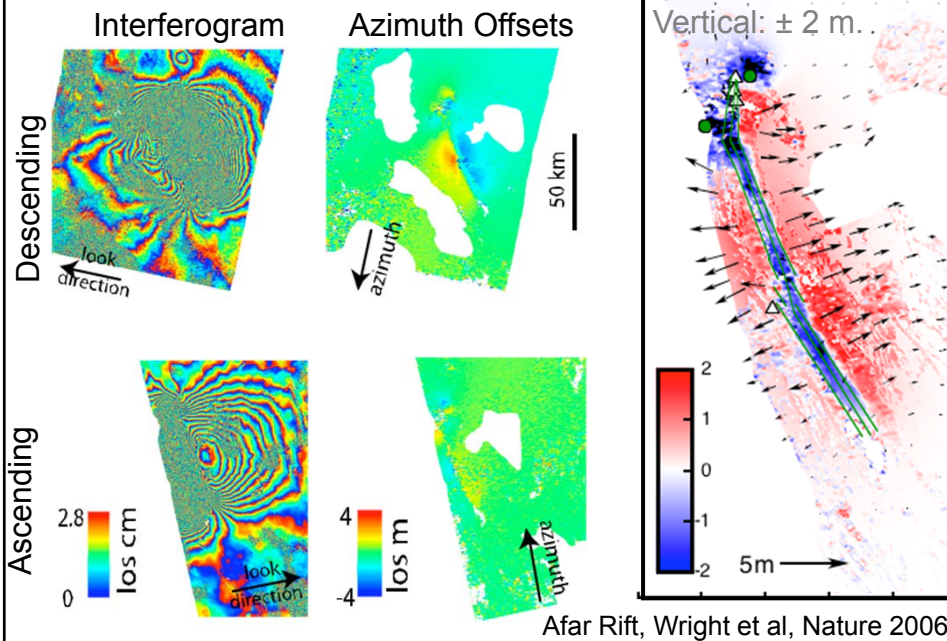
$\mathbf{d} = \mathbf{Lu}$, and solved for \mathbf{u} .

See e.g. Wright, T.J., B. Parsons, Z. Lu., Geophys Res. Lett. 30(18), p.1974, 2003

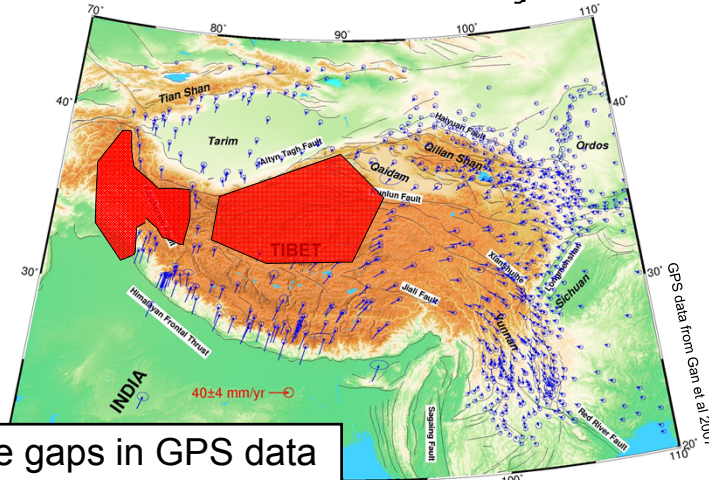
Bam earthquake 3D displacements



Combining Viewing Geometries

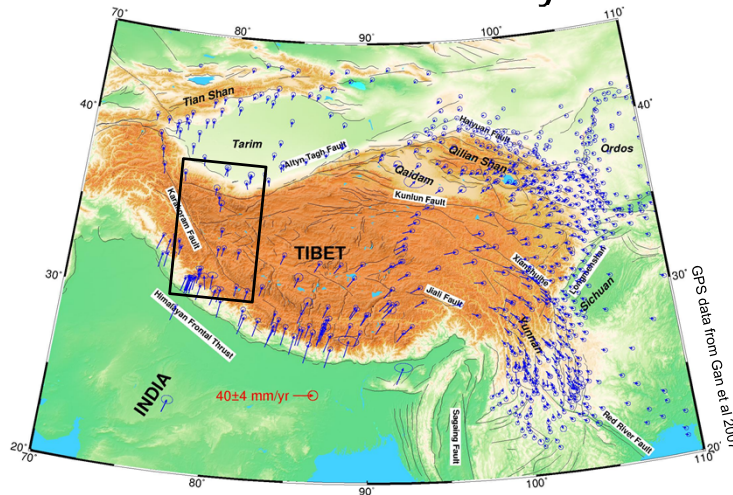


Tibet Case Study

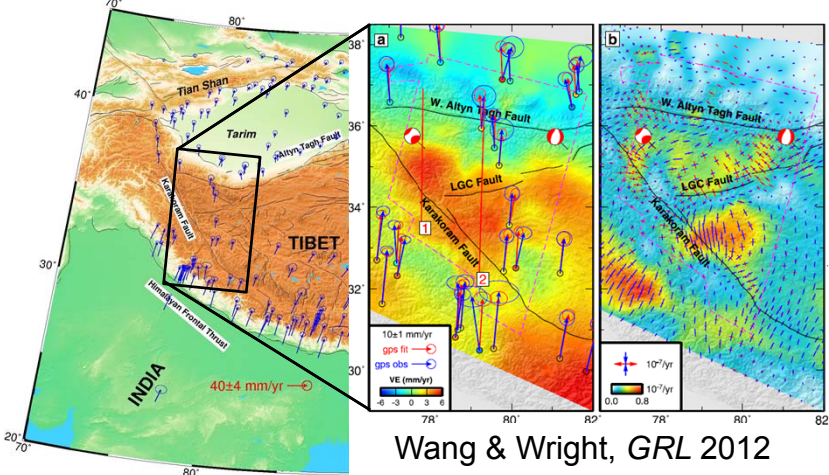


- Large gaps in GPS data
- Station spacing > 50 km

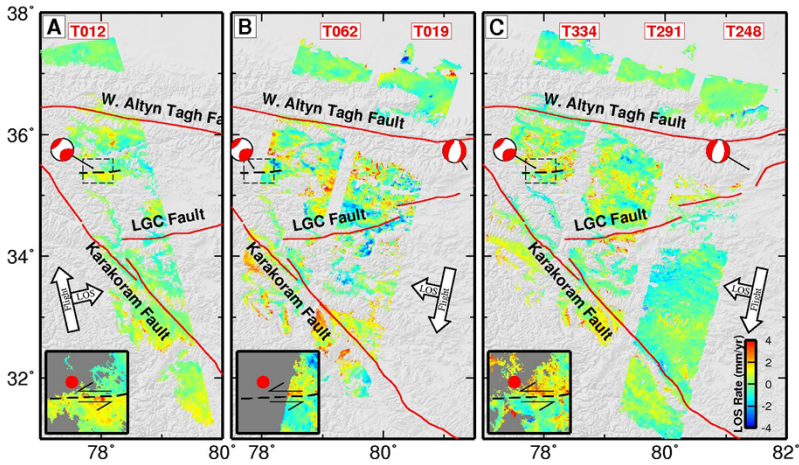
Tibet Case Study



Tibet Case Study

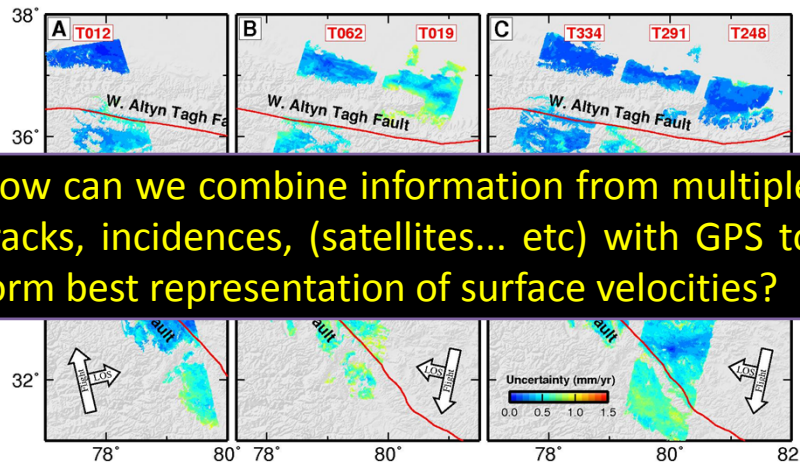


InSAR Rate Maps from PI-RATE



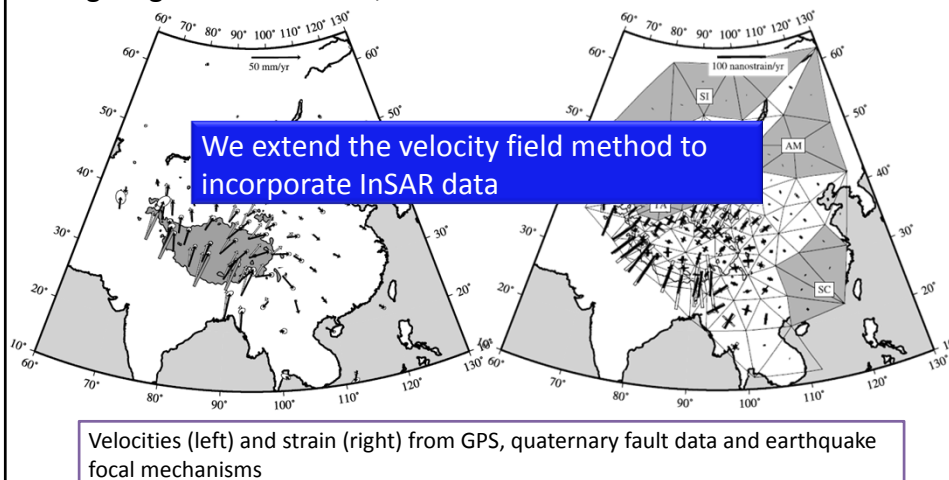
RATE MAP = DEFORM + ORB + ATM + NOISE

InSAR Error Maps from PI-RATE

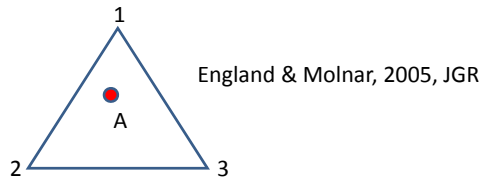
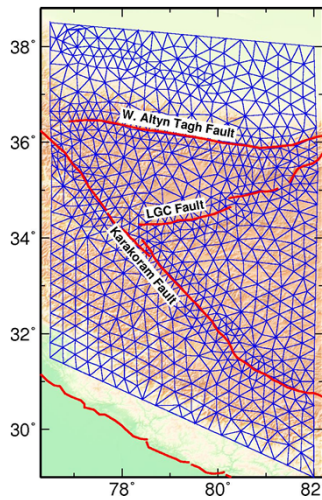


Velocity Field Method

e.g. England and Molnar, JGR 2005



Velocity Field Method: Mesh and Interpolation



England & Molnar, 2005, JGR

[24] We divide the surface of the region of interest into spherical triangles and assume that within each triangle, the velocity varies linearly with latitude and longitude across the triangle. We may express the velocity in the interior of the triangle in terms of the velocities of its vertices:

$$\mathbf{U} = \sum_{m=1}^3 N_m \mathbf{u}_m, \quad (5)$$

where \mathbf{u}_m is the velocity of vertex m and N_m are interpolation functions:

$$N_i = a_i + b_i \phi + c_i \theta, \quad (6)$$

where ϕ is longitude and θ is latitude.

Wang and Wright, GRL 2012

Velocity Field Method: LS Solutions

$$\begin{bmatrix} \mathbf{G}_{sar} & \mathbf{G}_{orb} & \mathbf{G}_{atm} \\ \mathbf{G}_{gps} & \mathbf{0} & \mathbf{0} \\ \mathbf{K}^2 \nabla^2 & \mathbf{0} & \mathbf{0} \end{bmatrix} \begin{bmatrix} \mathbf{M}_{vel} \\ \mathbf{M}_{orb} \\ \mathbf{M}_{atm} \end{bmatrix} = \begin{bmatrix} \mathbf{d}_{sar} \\ \mathbf{d}_{gps} \\ \mathbf{0} \end{bmatrix}$$

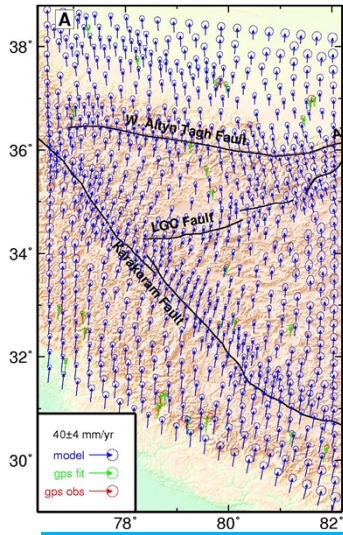
Weighted LS solution:

$$\hat{\mathbf{M}} = (\mathbf{G}^T \mathbf{W} \mathbf{G})^{-1} \mathbf{G}^T \mathbf{W} \mathbf{d}$$

Weighting by full data covariances

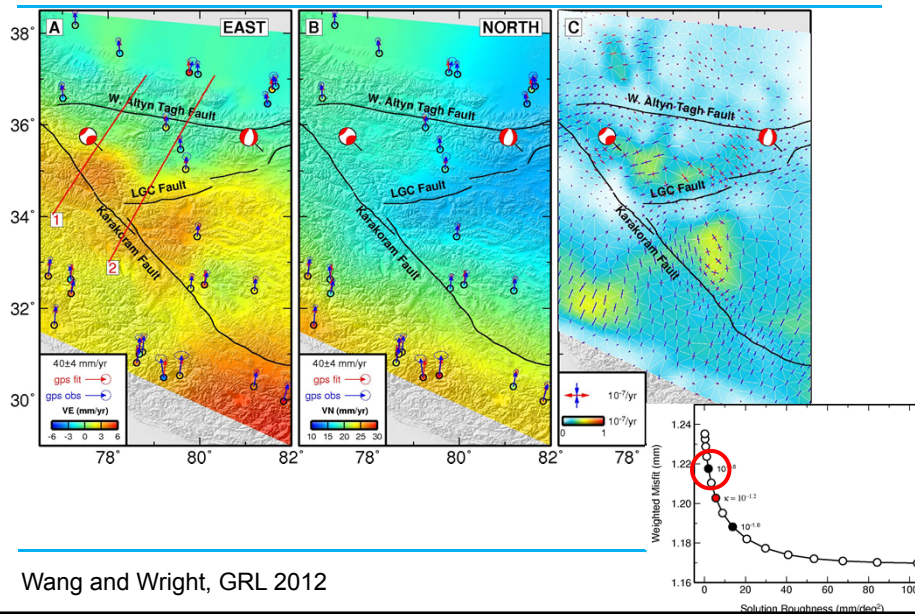
Wang and Wright, GRL 2012

Velocity Field: From Vertices to Continuous



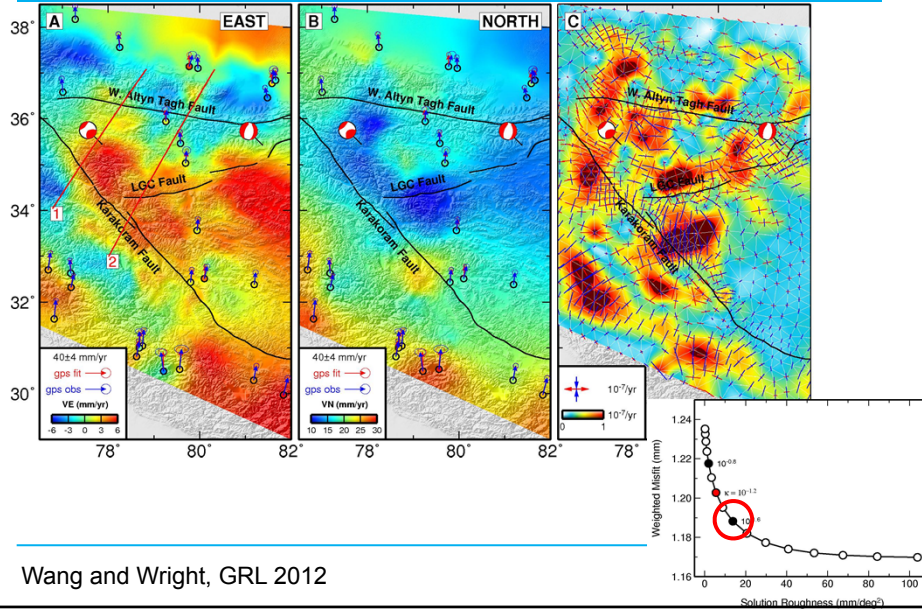
Wang and Wright, GRL 2012

Laplacian Smoothing: Over-smoothed



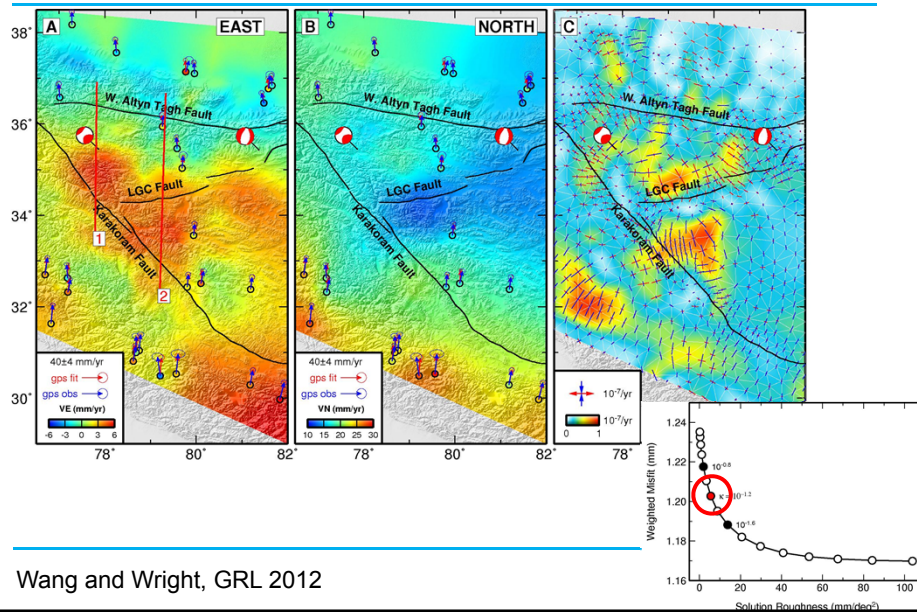
Wang and Wright, GRL 2012

Laplacian Smoothing: Little-smoothed



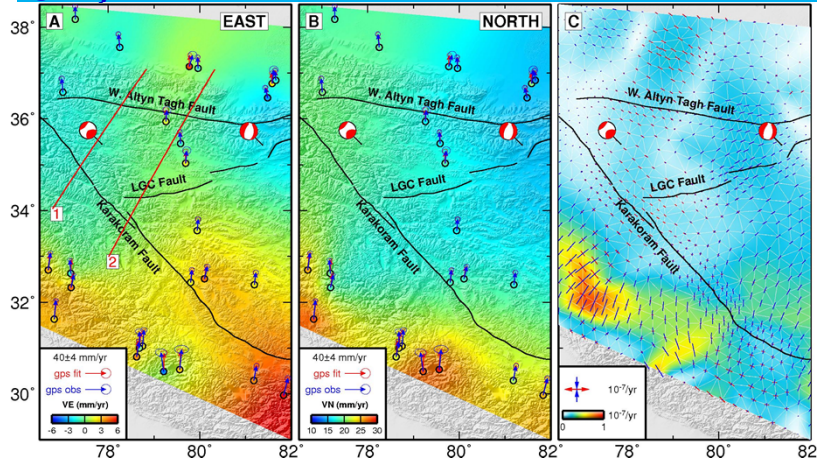
Wang and Wright, GRL 2012

Laplacian Smoothing: Best Solution



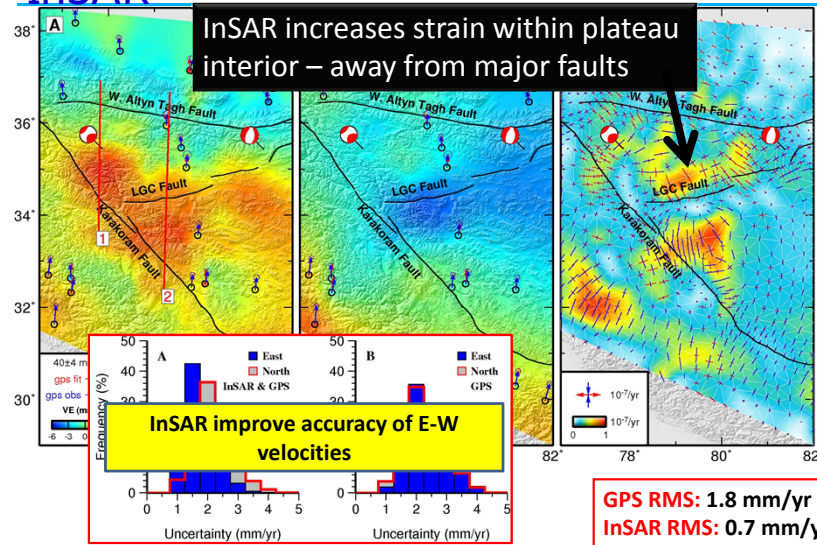
Wang and Wright, GRL 2012

Velocity & Strain Rate Field from GPS only



Wang and Wright, GRL 2012

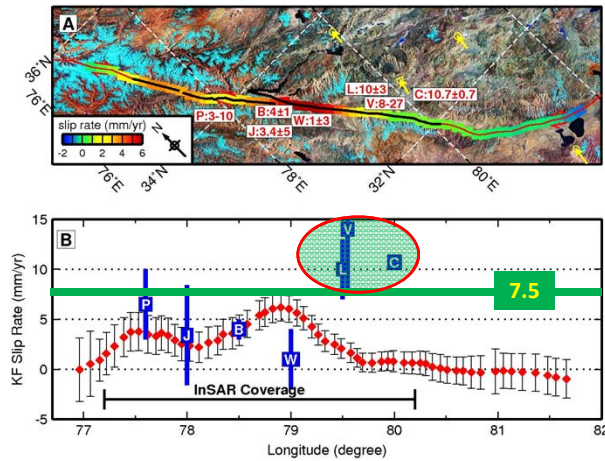
Velocity & Strain Rate Field from GPS & InSAR



Wang and Wright, GRL 2012

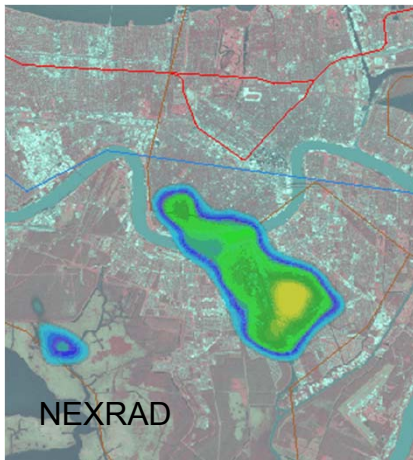
Slip Rates Along the Karakoram Fault

- Right-lateral slip along the entire fault
- Variable slip rate along the fault (0-6 mm/yr)
- Rule out present-day slip rates of >10 mm/yr
- No significant focused strain

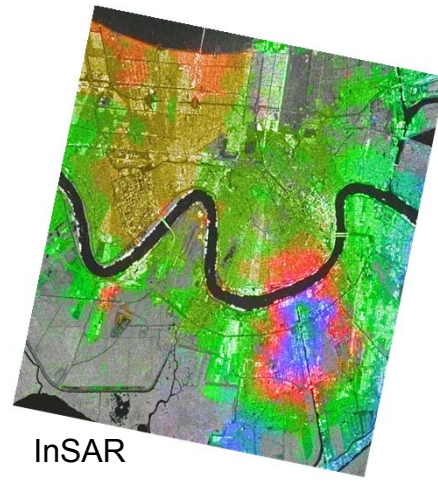


Limitation: Turbulent Atmosphere

Ground-based water vapour measurement

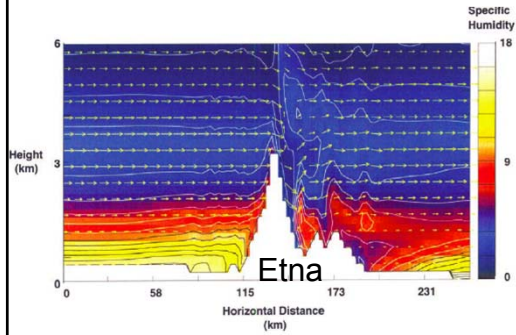
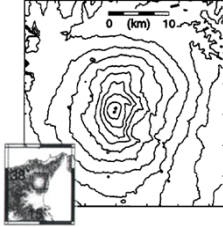


Interferogram

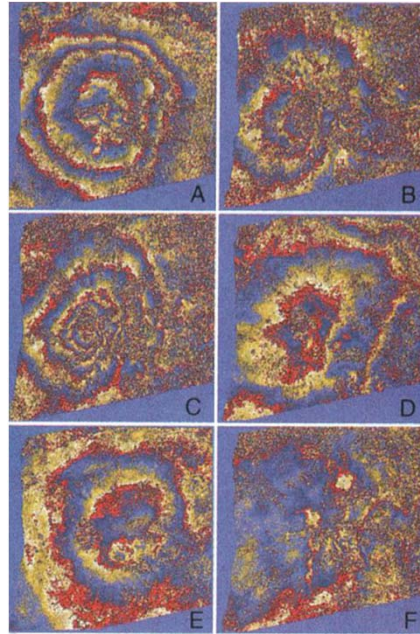


Limitation: Stratified Atmosphere

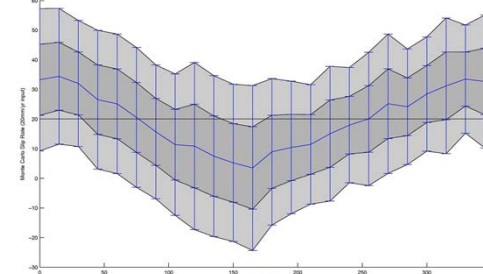
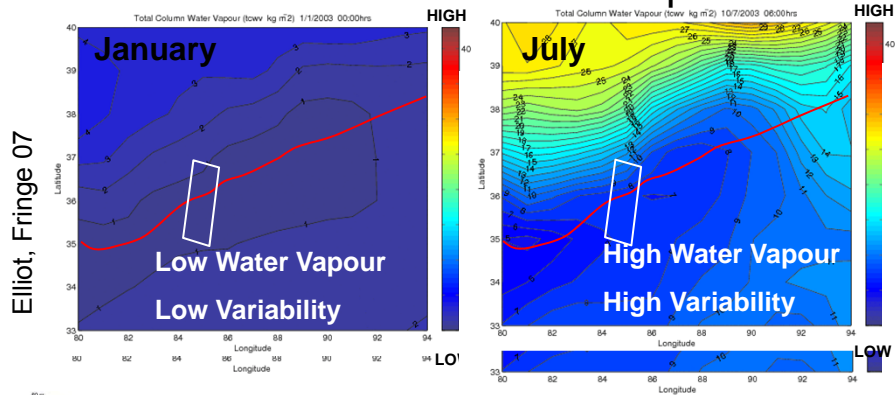
Mt Etna, Italy.



NH3D Model, Wadge 2002.



Limitation: Seasonal Atmosphere

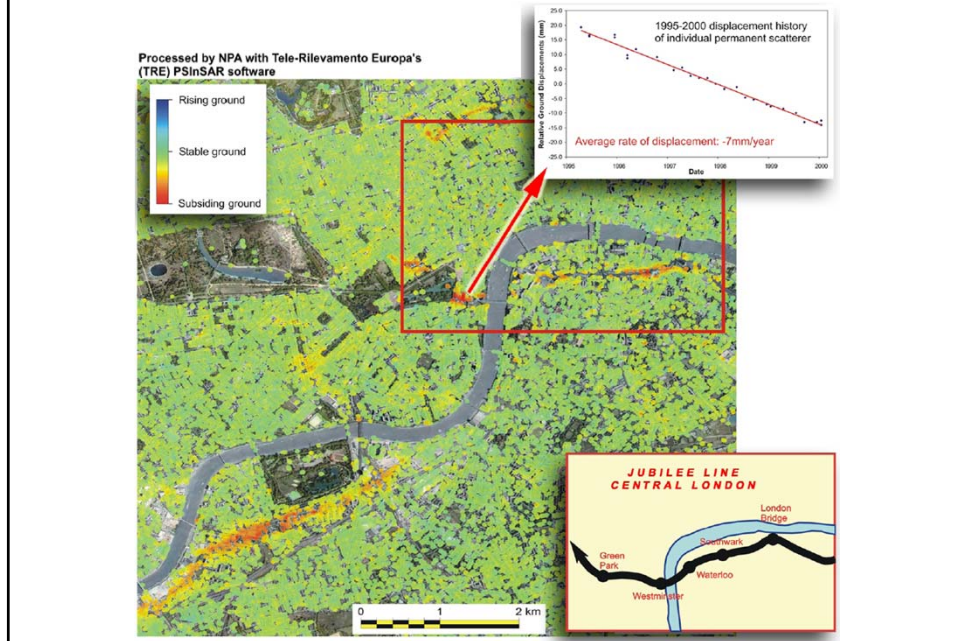


Synthetic Test of Rate Bias

Input Rate: 20 mm/yr

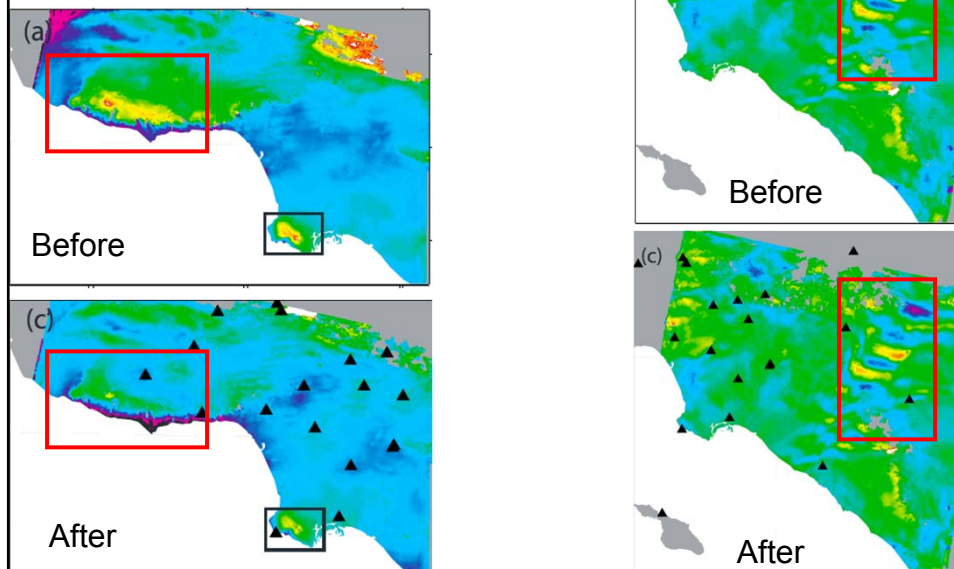
Recovered Rate: 5-35 mm/yr

Corrections 1: Linear/Smooth Velocity Assumption



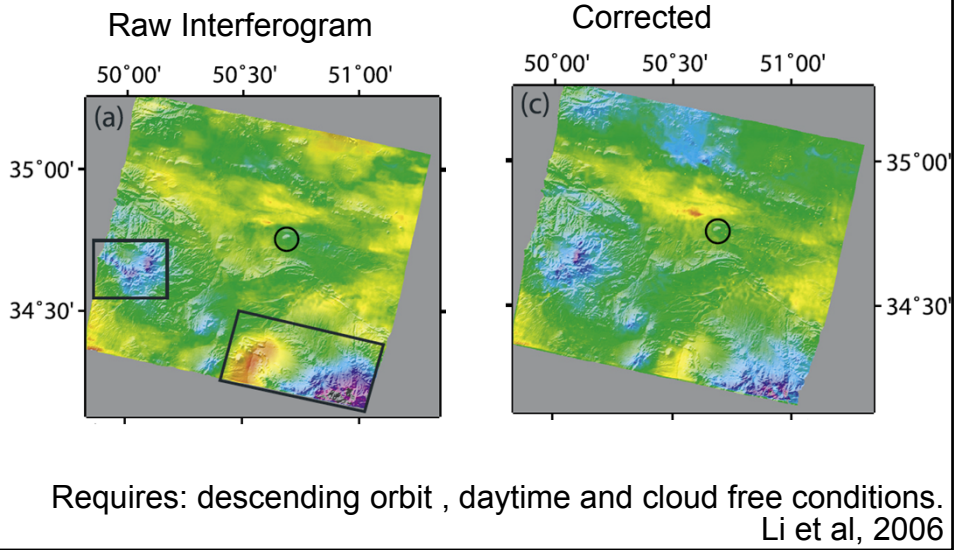
Correction 2: GPS

Requires dense GPS network
Li et al, 2006



Correction 3: MERIS (or MODIS)

Passive Optical/IR sensor on Envisat

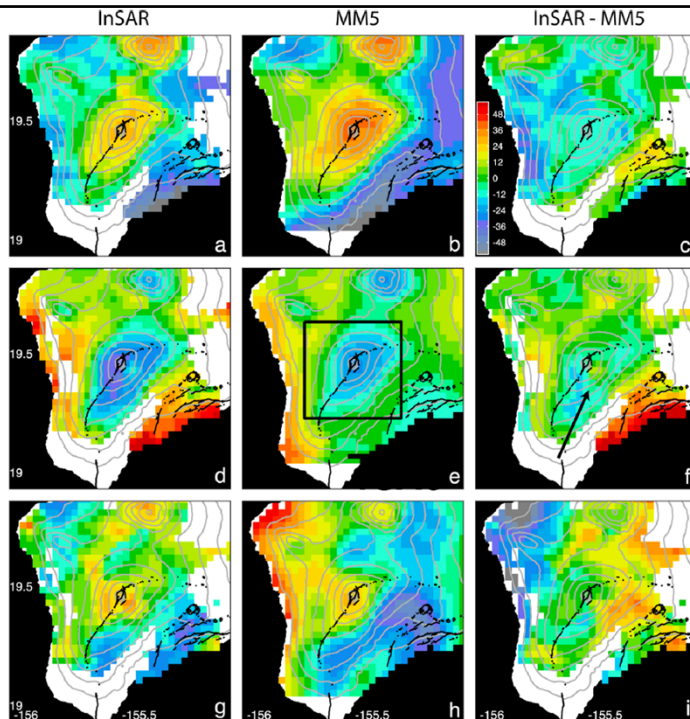


Atmospheric Correction 4: Weather Model.

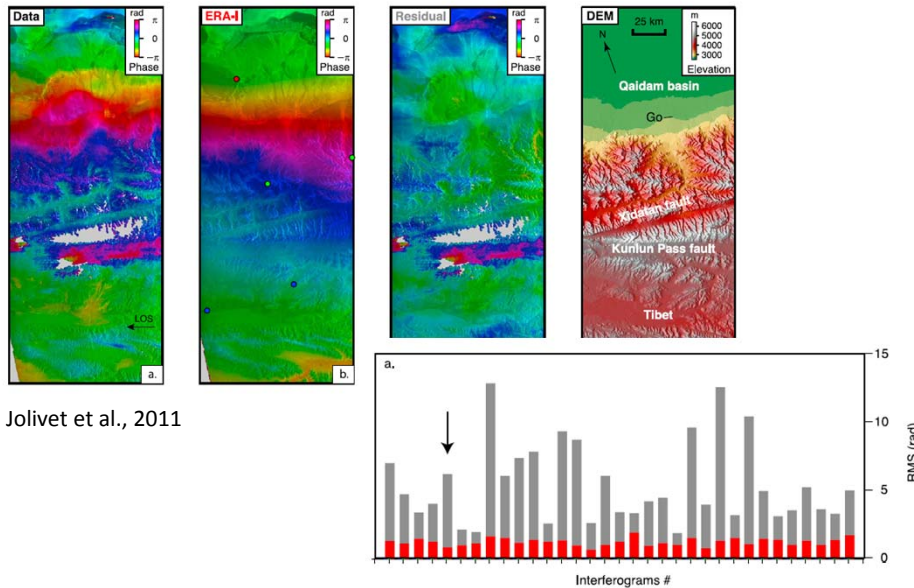
3 km resolution

Reduces long-wavelength (>30 km) effects but not smaller scale features.

Foster et al, 2006

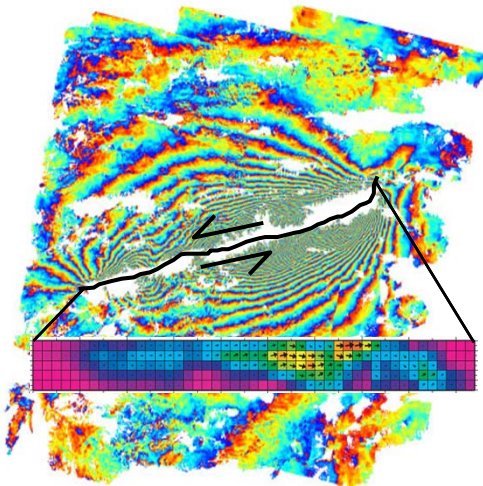


Atmospheric Correction 4: Weather Model (2)



Earthquakes

1. Coseismic Deformation



Current Capability

- Map deformation fields for most damaging earthquakes.
- Identify responsible faults
- Estimate slip models.
- Assess impact on future hazard .

What could be done?

- Routine analysis of ALL damaging earthquakes, c.f. Harvard CMT.
- Real-time assessment of causative fault and likely damage area.
- Near-real time assessment of future hazard (aftershocks + triggered quakes).

Why are we not doing this already?

- Data.
- Method Development.
- Manpower.

Earthquakes

2. Interseismic Strain

Current Capability

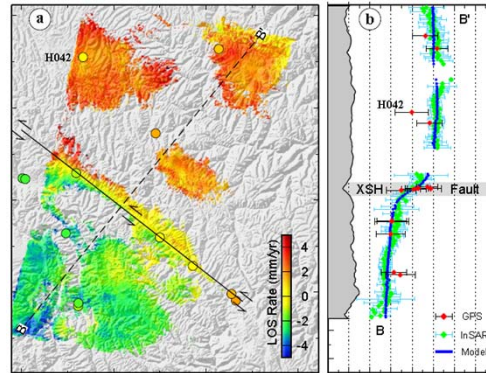
- Measure interseismic strain rates on suitable, targeted faults.
- Use these to constrain slip rate and hence assess future hazard.

What could be done?

- Routine measurement of strain across whole regions.
- Assessment of slip rates and relative hazard of multiple faults (including unidentified faults).

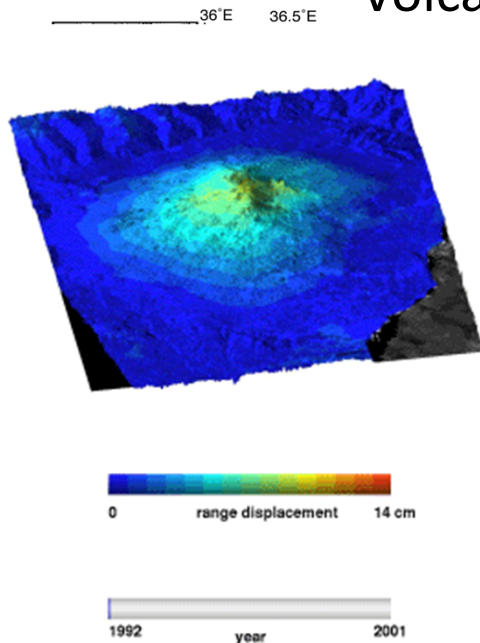
Why are we not doing this already?

- Data.
- Method Development.
- Manpower.



Wang, Wright and Biggs., GRL 2009

Volcanoes



Current Capability

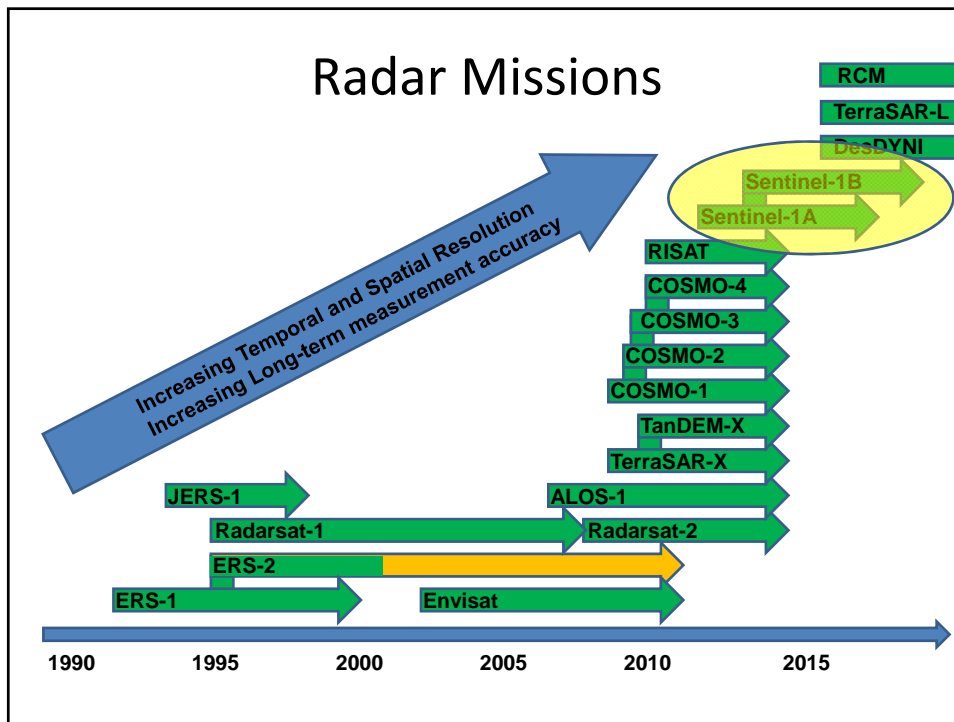
- Time-series analysis for suitable, targeted volcanoes .
- Snapshot regional surveys.
- Integration with other data sets.

What could be done?

- Routine monitoring of ALL volcanoes worldwide (or in a region).
- Target application of ground monitoring in countries where resources are limited.

Why are we not doing this already?

- Data.
- Method Development.
- Manpower.



The Future

Sentinel-1 (ESA, GMES)

- “Operational” C-band InSAR
- 12 day repeat, 2 satellites ⇒ 3 day revisit
- Funded for 20 years, Launch early 2014

© esa

Conclusions

- InSAR is a powerful, low-cost tool for monitoring Earth deformation
- Capability improving continuously (smaller rates, bigger areas...)
- Future missions and method development will ensure InSAR is a standard technique

